
Thermal Spray Processing of Nanoscale Materials—A Conference Report with Extended Abstracts*

C.C. Berndt and E.J. Lavernia

Significant interest has been generated recently in the field of nanoscale materials. This interest stems not only from the outstanding properties that can be obtained in such materials but also from the realization that early skepticism about the ability to produce high-quality, unagglomerated nanoscale powder was unfounded. There are many methods available to form nanocrystalline materials that can be further processed to evolve nanophase and or nanocrystalline structures. Some of these materials are becoming fully commercialized and, accordingly, the focus is shifting from synthesis to processing; that is, how to make useful coatings and structures from these powders. The potential applications span the whole spectrum of technology, for example, from thermal barrier coatings for turbine blades to wear-resistant rotating parts.

Significant progress has been made in various aspects of processing nanoscale materials. Most of this work is focused on the fabrication of bulk structures. However, the process most likely to have the earliest (and perhaps the greatest) major technological impact is deposition of coatings by thermally activated processes. This includes thermal spray methods such as HVOF and plasma spray, but also includes innovations such as chemical vapor condensation (CVC) and a number of exciting new combustion processes.

The objective of this conference was to assess the state-of-the-art in understanding the science and technology of thermally sprayed nanocrystalline coatings. The objective was accomplished by addressing the synergism between processing, physical and mechanical characteristics, and the behavior of these novel materials.

This conference was held in Davos, Switzerland, from 3-8 August, 1997. The Conference Chair was Professor Enrique J. Lavernia of the University of California at Irvine and the Conference Co-Chairs were Dr. Lawrence Kabacoff, Office of Naval Research, Arlington, Virginia, Dr. Manfred Rühle, Max-Planck-Institut für Metallforschung, Stuttgart, Germany, and Professor Koichi Niihara, Osaka University, Osaka, Japan. The "Thermal Spray Processing of Nanoscale Materials" conference was sponsored by The Engineering Foundation, New York, e-mail: engfnd@aol.com, <<http://www.engfnd.org>>.

*These extended abstracts have been edited to comply with a similar form and style. Figures have been numbered consecutively. References that are related to a single contribution are placed after each abstract, (that is, starting from "1") to facilitate continuity. Some authors have preferred to include a bibliography of key publications rather than specific references within the text.

1. Introduction to the Synthesis, Microstructure and Properties of Nanostructured Materials

H. Hahn, *Technological University of Darmstadt, Germany*,
hhahn@hrzpub.th-darmstadt.de

Nanostructured materials with microstructural features in the range of 2 to 50 nm have been studied for more than a decade. New synthesis techniques for nanopowders on a laboratory scale ranging from a few grams per day to an industrial scale on the order of tons per year have been developed (Ref 1). A wide range of techniques for the processing of nanostructured powders is available, including compaction, sintering, sinter forg-

ing, hot isostatic pressing, and so forth. An alternative route is thermal spray processing by which nanostructured coatings of conventional materials can be produced.

The basic research efforts have demonstrated that the properties of nanostructured materials are altered by grain size effects and due to the large volume fraction of internal interfaces. Mechanical (superplasticity, fracture, friction) (Ref 2), magnetic (Ref 3), electrical, catalytic, and optical properties have been found to be altered drastically at grain sizes below 20 nm. Additionally, the microstructural stability at temperatures above one-half their melting point is of interest because of the high

C.C. Berndt, SUNY at Stony Brook, New York, USA; cberndt@notes.cc.sunysb.edu; E.J. Lavernia, University of California at Irvine, California, USA; lavernia@uci.edu.

operating temperatures of devices. A large potential for application has been derived and several companies are actively involved in the exploration of these novel materials.

References

1. H. Hahn, Gas Phase Synthesis of Nanocrystalline Materials, *Nanostructured Mater.*, Vol 9 (No. 1-8), 1996, p 3-12

2. H. Hahn, P. Mondal, and K.A. Padmanabhan, Plastic Deformation of Nanocrystalline Materials, *Nanostructured Mater.*, Vol 9 (No. 1-8), 1996, p 603-606
3. T.A. Yamamoto, R.D. Schull, and H.W. Hahn, Magnetization of Iron-Oxide/Silver Nanocomposite by Inert Gas Condensation, *Nanostructured Mater.*, Vol 9 (No. 1-8), 1996, p 539-542

2. High Pressure Synthesis of Nanophase WC/Co/Diamond Powders: Implications for Thermal Spraying

B.H. Kear, Rutgers University, NJ, USA, bkear@rci.rutgers.edu, G. Skandan, Nanopowder Enterprises Inc., NJ, USA, 75031.1321@compuserve.com, and R. Sadangi, Diamond Materials Inc., NJ, USA, diamat@aol.com

A method has been developed for the synthesis of nanophase WC/Co/diamond powders, which consist of a high volume fraction of diamond in a WC/Co matrix. Starting with high surface area WC/Co powder (available from Nanodyne Inc.), the process involves (1) chemical vapor infiltration (CVI) of the porous WC/Co powder with amorphous or graphitic carbon, and (2) high-pressure/high-temperature (HPHT) transformation of the carbon-infiltrated WC/Co powder to nanophase WC/Co/diamond powder. In the critical CVI step of the process, the kinetics of the carbon deposition must be controlled to achieve uniform

deposition throughout the porous WC/Co powder particles. Although the details must be worked out, this new class of powders should make useful feedstocks for thermal spraying, at least using the HVOF process, where the peak temperature in the flame and the particle residence time can be adjusted to avoid significant graphitization of the diamond phase during spraying. A triphasic superhard coating should display superior wear resistance, making it an attractive candidate coating material for wear parts and machine tools.

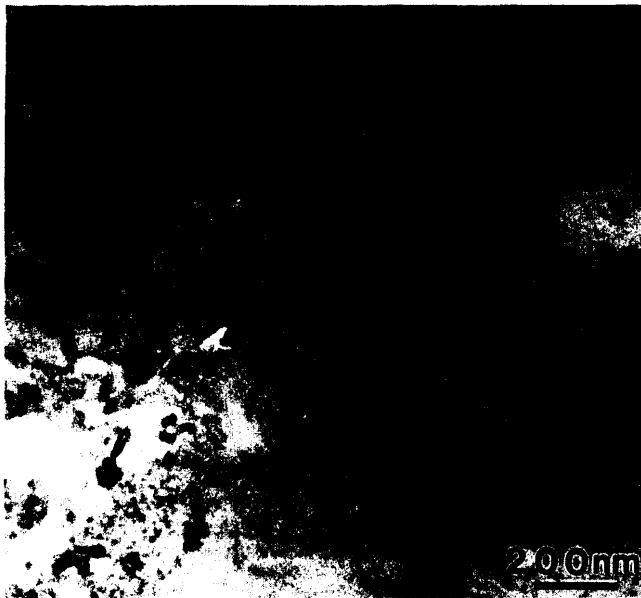
3. Synthesis of Nanostructured Engineering Coatings by High Velocity Oxygen Fuel (HVOF) Thermal Spraying

H.G. Jiang, M.L. Lau, and E.J. Lavernia, University of California at Irvine, CA, USA, lavernia@uci.edu

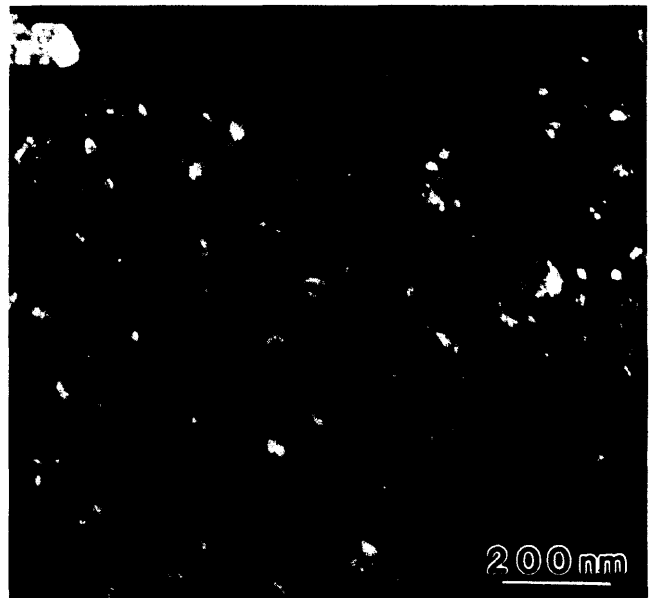
Thermal spray processes, such as plasma and HVOF techniques, have evolved into sophisticated and practical methods for the synthesis of engineered coatings. In particular, HVOF thermal spraying has attracted commercial interest for its ability to produce coatings that combine high hardness and bond strength with minimal porosity, tailored thickness, and surface roughness. In recent years, HVOF thermal spraying has been used to fabricate nanostructured coatings using nanocrystalline powder feedstock prepared by mechanical alloying/milling or chemical synthesis. The relatively low temperatures and short dwell time that the powder particles experience during HVOF thermal spraying help to preserve the nanocrystalline structure in the final coatings.

High-velocity oxyfuel spraying combines complex processes of combustion and gas dynamics (including fluid and particle dynamics) and particle flattening and solidification on the

substrate surface to form a coating. The dynamic processes are further complicated for the thermal spraying of nanocrystalline materials as the particle morphology deviates from the conventional spherical powders used for thermal spraying. Recently, nanocrystalline Ni, Inconel 718, and 316 stainless steel feedstock powders prepared by methanol or cryogenic milling were thermally sprayed using a Sulzer Metco DJ 2600 HVOF system and the resulting coatings found to remain nanocrystalline. Transmission electron microscopy performed on the methanol milled Ni powders for 10 h indicates the presence of nanocrystalline grains with an average grain size of 82 nm. Figure 1 shows regions of nanocrystalline grains on the cross section of the methanol milled Ni (10 h) coating in which areas with a grain size ranging from 100 to 200 nm and elongated grains with an aspect ratio of 2 to 3 were observed. The presence of these elongated grains resulting from the mechanical milling process sug-



(a)



(b)

Fig. 1 (a) Bright field image of methanol-milled nickel (10 h) cross-sectional coating. (b) Dark field image of methanol-milled nickel (10 h) cross-sectional coating

gests that fractions of the nanocrystalline agglomerates did not melt during the **HVOF** spraying. Microhardness measurements performed on the nanocrystalline Ni, **Inconel** 718, and 316 stainless steel (methanol milled for 10 h) coatings yield values that are approximately 20, 60, and 36 percent, respectively, higher than those of conventionally sprayed coatings when air was used as a carrier gas during thermal spraying. Furthermore, the hardness values increase with increasing aspect ratio, which suggests that the morphology of the particles influences the properties of the coatings. Further study is underway to investigate this phenomenon.

Selected References

- J.-P. Delplanque, E.J. Lavernia, and R.H. Rangel, "Description of a Micro-Pore Formation Mechanism in a Deforming and Solidifying Metal Droplet," presented in the 1995 ASME Winter Annual Meeting (San Francisco, CA) American Society of Mechanical Engineers, 1995
- J.-P. Delplanque, E.J. Lavernia, and R.H. Rangel, "Multidirectional Solidification Model for the Description of Micropore Formation in Spray Deposition Processes," *Numer. Heat Transfer; A*, Vol 30, 1996, p 1-17
- E.J. Lavernia, H.G. Jiang, and M.L. Lau, "Thermal Spray Processing of Nanocrystalline Materials," presented at NATO Advanced Study Institute (ASI) on Nanostructured Materials: Science and Technology (St. Petersburg, Russia), 11-20 Aug 1997
- T.S. Srivatsan and E.J. Lavernia, Review—Use of Spray Techniques to Synthesize Particulate-Reinforced Metal-Matrix Composites, *J. Mater. Sci.*, Vol 27, 1992, p 5965-5981
- V. Tellkamp, M.L. Lau, A. Fabel, and E.J. Lavernia, Thermal Spraying of Nanocrystalline **Inconel** 718, *Nanostructured Mater.*, Vol 9, 1997, p 489-492

4. Thermal Spray Processing of Nanoscale Materials by HVOF/HVIF

P.R. Strutt, Inframat Corporation, CT, USA

One distinctive feature of nanostructured materials is hardness enhancement combined with good fracture toughness (Ref 1, 2). Insight into the strength of WC-Co nanomaterial has been demonstrated where hardness values of 2200 to 2300 VHN were obtained in a 10% Co liquid-phase-sintered material. This contained alloying additions for solid-solution strengthening, car-

bide-matrix wetting, and grain growth inhibition. Such discoveries in a bulk nanomaterial clearly hold promise for thermally spraying nanostructured coatings. In pursuing this applications area, Inframat has built upon developments made at the Precision Manufacturing Center at the University of Connecticut (Ref 3).

Table 1 lists successive developments in thermally spraying *n*-WC/Co. Initially, as-synthesized powder (produced by Nanodyne Corporation, New Brunswick, NJ) was used as feed-stock. In this material, a WC-Co nanocomposite constitutes the shell of a 50 μm diam hollow particle (Fig. 2a). To improve coating density and increase hardness, solid agglomerated particles were produced by ultrasonic disintegration of the hollow shells into nanocomposite fragments (Fig. 2b), followed by reconstitution (Fig. 2c), using a spray dry technique. As shown in Table 1, spraying in a nitrogen shroud gas and adding sacrificial carbon to the reconstituted particles did not achieve a hardness increase, although WC decomposition was reduced. A further increase in hardness was obtained using the hyperimpact fusion gun (Ref 4) to produce a higher particle velocity. However, the highest hardnesses (1650 to 1900 VHN) were obtained by dc plasma arc deposition, using reconstituted nanopowders containing proprietary alloying additions to improve solid-solution strengthening, matrix-particle wetting, and grain-growth inhibition.

Overall, studies on WC-Co coatings show that substantially higher hardnesses are obtained using nanomaterial; however, regions with considerable porosity exist throughout these coatings. This is evident in Fig. 3(a), which shows extensive porosity in the lower right-hand corner; however, slightly away in a non-porous region a diamond indentation reveals the hardness to be 1720 VHN. Examination of the morphology at higher magnification reveals a microstructure similar to that in Fig. 3(b), which is for liquid-phase-sintered material.

Clearly, considerable structural coarsening is evident in Fig. 3(b) because the grain size of the original powder was 30 nm; nevertheless, the high microhardness is impressive (2200 VHN). Thus, some degree of structural coarsening is not detrimental in obtaining high hardnesses. Also, it appears that hardness is not significantly reduced by partial WC phase decomposition during thermal spraying. Consequently, porosity is the critical factor in determining nanostructured coating performance. This conclusion shows the importance of (1) minimizing residual porosity in nanoparticle feed powder and (2) quantifying how thermal spray conditions determine coating density. In addressing (1) and (2) above Inframat is currently optimizing the thermal spray properties of agglomerated nanopowders. This requires being able to produce powders with (1) narrow particle size distribution, (2) high particle density (low porosity), and (3) high particle strength. This involves paying attention to spray drying parameters and also the selection of appropriate polymeric binders, deflocculants, defoaming agents, and agents determining the degree of hydrolysis, and the isoelectric point.

In addition to reprocessing hollow shell *n*-WC/Co material, another processing route is to chemically synthesize highly dispersed nanoparticle suspensions of ceramic materials, including yttria-stabilized zirconia. In this case, a distinct advantage is the assembly of individual ceramic nanoparticles into an agglomerated particle; see Fig. 2(d) and (e). This clearly produces a denser agglomerated particle than the assembly of nanocompo-

Table 1 Thermal spraying of nanostructured WC-Co

Year	Gun	Powder type	Spraying environment	Hardness, VHN	Phases present
1993	Metco Diamond Jet	Hollow shells	Air	1050-1200	WC, W ₂ C, W
1994	Metco Diamond Jet	Solid particles	Air	1200-1350	WC, W ₂ C, W
1995(a)	Metco Diamond Jet	Solid particles	N ₂ shroud	1200-1350	WC, W ₂ C, W
1996	Metco Diamond Jet	Solid particles + C	N ₂ shroud	1200-1350	WC, W ₂ C, W
1996	Browning	Solid particles	Air	1600	WC
1996	Tafa JP-5000	Solid particles	Air	1350-1500	WC, W ₂ C, W
1997	Metco 9MB plasma gun	Solid particles + additive	Air	1650-1900	WC, W ₂ C, W

(a) Patent application

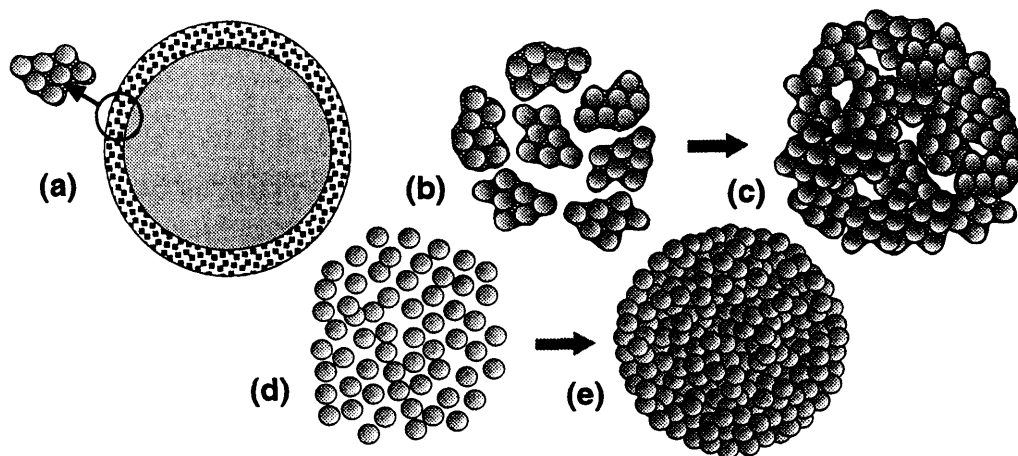


Fig. 2 Processing nanocomposite shells (a) to (c) and dispersed nanoparticles (d) and (e) into thermal spray agglomerates. Note that (d) and (e) minimize agglomerate porosity compared with (a) to (c).

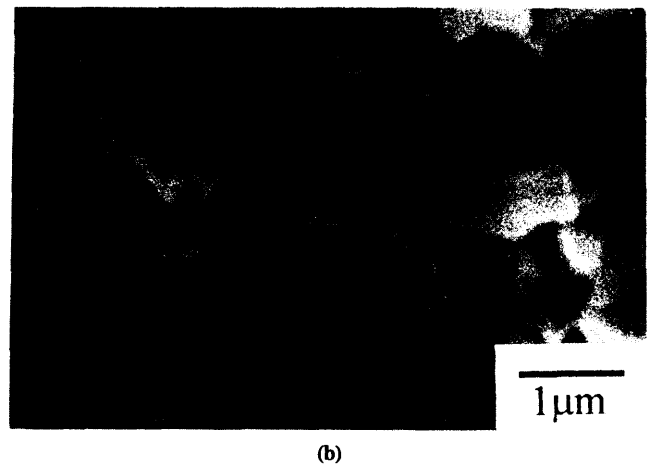
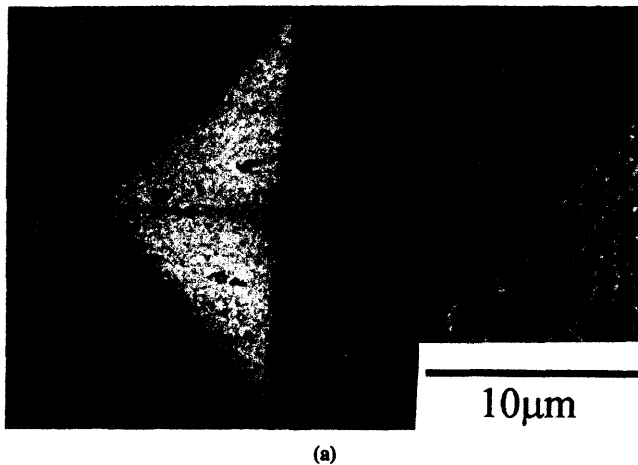


Fig. 3 (a) Nanostructure in WC-10%Co liquid phase sintered material containing propriety additives with a hardness of 2200 VHN. (b) Diamond indentation in thermally sprayed coating with a hardness of 1720 VHN. Note the significant porosity adjacent to the indentation.

site fragments (formed by disintegrating hollow shell material), as depicted in Fig. 2(a) to (c).

References

1. B.H. Kear and L.E. McCandlish, Chemical Processing and Properties of Nanostructured WC-Co Materials, *Nanostructured Mater.*, Vol 3 (No. 1-6), 1993, p 19-30
2. B.H. Kear and P.R. Strutt, Nanostructures: The Next Generation of High Performance Bulk Materials and Coatings, *Naval Res. Rev.*, Vol 46 (No. 4), 1994, p 4-13
3. P.R. Strutt, R.F. Boland, and B.H. Kear, "Nanostructured Feeds for Thermal Spray Systems, Methods of Manufacture, and Coatings Therefrom," U.S. Patent, filed Nov 1995
4. J.A. Browning, Hypervelocity Impact Fusion—A Technical Note, *J. Therm. Spray Technol.*, Vol 1 (No. 4), 1992, p 289-292

5. Thermal Spray Processing of Nanophase Co/WC and Ni-Base Alloys

E. Strock, Engelhard Corporation, CT, USA, elaine.strock@engelhard.com

Commercial applications for thermal sprayed coatings containing nanoscale phases take advantage of their unique combinations of properties compared to conventional coatings. Improved toughness of tungsten carbide coatings without loss of wear resistance, improved wear resistance of oxidation-resistant metallic coatings, and improved oxidation resistance of chromium carbide coatings are among the desired changes in thermal spray coatings that may be provided by nanoscale materials.

Thermal spray coatings of WC/Co- and Ni-base nanophase powders were produced using several types of HVOF torches to

determine the spray characteristics of metals and gain some understanding about their sensitivity to torch and parameter changes. Although the WC/Co material was applied initially with three different torches (JetKote, Diamond Jet, and JP-5000), most experiments were performed with the Diamond Jet torch. These studies examined the effect of spray parameters on hardness, roughness, and microstructure as well as observations concerning the powder feeding and sample temperature.

6. Nanostructured Products: Development and Potentials for Nanostructured Powders

M.L. Trudeau, Hydro-Québec Research Institute, Québec, Canada, trudeaum@ireq.ca

The field of nanostructured materials is at a crossroad. Since its emergence more than 10 years ago, new materials with exciting properties have been discovered (Ref 1, 2). For instance, im-

pressive technological potential was demonstrated in magnetism, catalysis (Ref 3), hydrogen storage (Ref 4), and in the improvement of electrical contact (Ref 5). However, since the

beginning of this field it was recognized that for it to really mature rapidly and be used in large-scale industrial applications, two major problems had to be solved. First is the large-scale production of materials, and this has been addressed by a number of techniques. For example, one synthesis process that demonstrated its potential for large-scale production is high-energy mechanical milling (HEMM) (Ref 6, 7). HEMM has been used extensively for the past ten years to produce various **nanostuctured** or nanocomposite materials. Structural changes occurring during high-energy milling are substantial with many parameters involved; for instance, powder-to-ball weight ratio, the number and size of the balls, the energy intensity, and the milling temperature and atmosphere.

Macroscopically, a **three-stage** process for the formation of nanostructure by high-energy milling was presented by Fecht (Ref 8).

- Localized deformation occurs in shear bands containing a high dislocation density. The **atomic-level** strain can increase up to 3%.
- The dislocations are annihilated and recombine to establish small-angle grain boundaries creating a **subgrain** structure of nanoscale dimensions.
- The orientation of grains with respect to their neighboring grains becomes completely random.

The particulates produced by HEMM are normally agglomerates with dimensions between 5 to 50 μm . On the other hand, the average size of the crystallites forming these agglomerates can be reduced down to about 10 nm. One of the main advantages of HEMM is that this process can be scaled up to produce tonnage quantities of materials.

The second difficulty is more complex and relates to the fact that, indeed, most synthesis processes produce powders or agglomerates composed of nanosized crystals. For most industrial applications, except in fields where only surface reactivity is important, such as in catalysis or for hydrogen storage, these powders need to be **densified** without the loss of their nanostructure to obtain bulk products. Based on the preliminary results obtained on small quantities of nanostructured materials, there is large interest from industry to develop new products using such powders for applications such as more efficient electrocatalytic

electrodes, **wear-** and corrosion-resistant coatings or more efficient magnetic materials, if such densification processes can be developed successfully.

At the present time, in order to sustain the research interest there is an urgent need to move from the small-scale laboratory design to large-scale production capability. Thermal spray techniques can produce dense coatings or products if the structures **and/or** the chemical compositions of the nanostructured precursors can be retained. Some areas of present interest for **Hydro-Québec** are in the manufacture of more efficient and mechanically stable electrical contacts and in the development of **cavitation-resistant** coatings. It is, thus, crucial to develop a synergy between all the different research **fields**, from powder development to product design, in order to push the potential of nanostructured materials to a larger scale of industrial applications.

References

1. See for example the Proceeding of the Third International Conference on Nanostructured Materials, *Nanostructured Mater.*, Vol 9, 1997
2. M.L. Trudeau, Nanostructured Materials: Some Physical Considerations, *J. Phys., Condens. Mater.*, in print
3. M.L. Trudeau and J.Y. Ying, Nanocrystalline Materials in Catalysis and Electrocatalysis: Structure Tailoring and Surface Reactivity, *Nanostructured Mater.*, Vol 17 (No. 1/2), 1996, p 245-258
4. L. Zaluski, A. Zaluska, P. Tessier, J.O. Strom-Olsen, and R. Schulz, Hydrogen Absorption by Nano-crystalline and Amorphous Fe-Ti with Palladium Catalyst Produced by Ball Milling, *J. Mater. Sci.*, Vol 31, 1996, p 695-698
5. M.L. Trudeau, K. Bryden, M. Braunovic, and J.Y. Ying, Fretting Studies of Nanocrystalline Pd, Pd-Ag, and Pd-Y Films, *Nanostructured Mater.*, Vol 9, 1997, p 759-762
6. C.C. Koch, Synthesis of Nanostructures by Mechanical Milling: Problems and Opportunities, *Nanostructured Mater.*, Vol 9, 1997, p 13-22
7. M.L. Trudeau, Nanostructured Materials Produced by High Energy Mechanical Milling and Electrodeposition, *Proc. of the NATO Workshop on Nanostructured Materials* (St. Petersburg, Russia), 11-21 Aug 1997, in press
8. H.J. Fecht, *Nanophase Materials by Mechanical Attrition: Synthesis and Characterization*, NATO ASI series E-Vol 260. G.C. Hadjipanayis and R.W. Siegel, Ed., 1994, p 125-144

7. Combustion Flame-Chemical Vapor Condensation: A New Technology for Production of Nanostructured Powders and Coatings

G. Skandan and E. Heims, Nanopowder Enterprises Inc., NJ, USA,
75031.1321@compuserve.com, and N. Glumac, Y.J. Chen, F. Cosandey,
and B.H. Kear, Rutgers University, NJ, USA

Sprayable nanopowders are needed for the formation of nanostructured coatings. Previous work (Ref 1-3) has shown that gas condensation processing using chemical precursors as the starting materials yields loosely agglomerated nanoparticles in the 3 to 50 nm size range that have uniform particle size **distrib-**

ution. The process called chemical vapor condensation (CVC) is continuous and amenable to scale-up. It combines rapid thermal decomposition of a **precursor/carrier** gas stream in a reduced pressure environment with thermophoretically driven deposition of the rapidly condensed product species on a cold

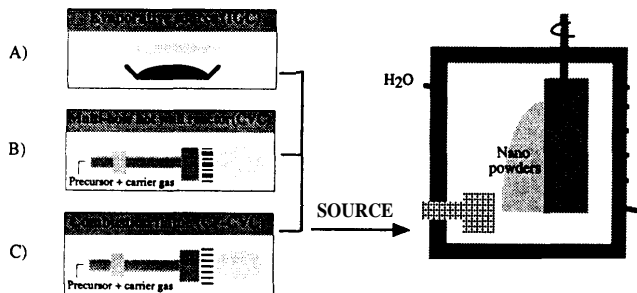


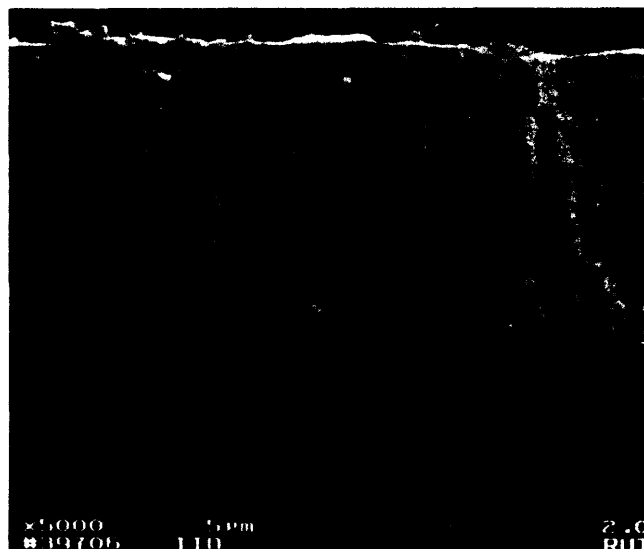
Fig. 4 Evolution of the chemical vapor condensation (CVC) process. A, evaporation source for producing metallic powders; B, hot-wall reactor source for producing carbides and nitrides; C, flat-flame combustor for oxide powders

substrate. Recently, (Ref 4, 5) the hot-wall reactor in the system has been replaced with an efficient heat source—a low-pressure flat-flame combustor—thereby increasing the production rate by two orders of magnitude. The modified process, called combustion flame-chemical vapor condensation (CF-CVC), has been used to produce loosely agglomerated nanoparticles of SiO_2 , TiO_2 , Al_2O_3 , SnO_2 , and $\text{In}_2\text{O}_3\cdot\text{Sn}$. The combustor is more than just a heat source for precursor pyrolysis; because the high concentration of OH radicals in the low-pressure flat flame aids in the decomposition kinetics (Ref 6). The evolution of the process is shown in Fig. 4. The present prepilot scale reactor is equipped with a burner that is 13 cm in diameter and is capable of producing powders at the rate of ~ 300 g/h.

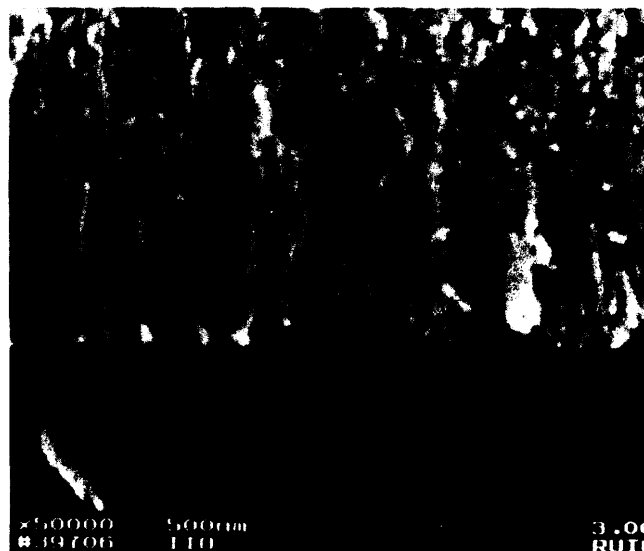
Instead of producing powders first, and forming coatings subsequently, a one-step process that completely avoids the use of powders as a starting material could be beneficial in terms of significant cost reduction, as well as the ability to easily access the critical thickness range of 1 to 10 μm that is difficult by conventional coatings technologies. For example, thin-film deposition processes have low deposition rates, ~ 1 $\mu\text{m}/\text{h}$, and thick-film deposition techniques are not particularly suited to such film thicknesses. The cold substrate, which was used to quench the nanoparticles, has been replaced by a heated substrate. "Superheated" nanoparticles condensing from the gas phase impinge upon the heated substrate and sinter to form a coating. Either porous or dense adherent films, with nanoscale features in both cases, are formed by altering the processing parameters, such as substrate temperature and flame temperature profile. Figure 5(a) shows a SnO_2 film deposited on a quartz substrate at low magnification, and 5(b) of the figure shows the "nanoporous" nature at high magnification. High deposition rates of ~ 1 $\mu\text{m}/\text{min}$ are achieved because the film is formed from deposition of nanoparticles, as opposed to molecules, which is the case with chemical vapor deposition (CVD). The initial impact velocity is sufficient to form necks between the particles, which is the initial stage of sintering, and the large curvature resulting from a very small grain/particle size provides a large driving force for sintering. Furthermore, the nanoparticles are in pristine condition as they impinge upon the substrate, thus making densification relatively easy.

References

1. W. Chang, G. Skandan, H. Hahn, S.C. Danforth, and B.H. Kear, Chemical Vapor Condensation of Nanostructured Ceramic Powders, *Nanostructured Mater.*, Vol 14 (No. 3), 1994, p 345-351



(a)



(b)

Fig. 5 (a) SnO_2 film deposited on a quartz substrate at low magnification. (b) "Nanoporous" nature at high magnification. (Art has been reduced to 97% of its original size for printing.)

2. B.H. Kear, W. Chang, G. Skandan, K. Kan, S.C. Danforth, and H. Hahn, Synthesis of Ceramic Powders and Whiskers from Chemical Precursors, *Proc. TMS Meeting on Novel Techniques in Synthesis and Processing of Advanced Materials*, J. Singh and S.M. Copley, Ed., 1995, p 261-270
3. G. Skandan, N. Glumac, Y.-J. Chen, J.J. Lin, R. Rittmann, and B.H. Kear, Vapor Phase Synthesis and Consolidation of Nanophase Oxides, *Proc. TMS Meeting on Synthesis and Processing of Nanocrystalline Powder*; D. Bourell, Ed., 1996, p 81-87
4. Y.-J. Chen, N. Glumac, G. Skandan, and B.H. Kear, High Rate Synthesis of Nanophase Materials, *Nanostructured Mater.*, Vol 9 (No. 1-8), 1997, p 101-104
5. N. Glumac, Y.-J. Chen, G. Skandan, and B.H. Kear, Scalable High-Rate Production of Non-agglomerated Nanopowders by Flame Synthesis, *Mater. Lett.*, in press
6. N. Glumac, Y.-J. Chen, and G. Skandan, Diagnostics and Modeling of Nanopowder Synthesis in Low Pressure Flames, *J. Mater. Res.*, in press

8. Microstructure Development and Control During Plasma Spray Deposition

S. Sampath and H. Herman, SUNY at Stony Brook, NY, USA,
ssampath@ccmail.sunysb.edu

Plasma spray processing is a well-established method for forming protective coatings and free-standing shapes of a wide range of alloys and ceramics. It is a complex process, involving rapid melting and high-velocity impact deposition of powder particles. Due to the rapid solidification nature of the process, deposit evolution is complex, commonly leading to ultrafine-grained and metastable microstructures. The properties of a plasma sprayed deposit are directly related to this complex microstructure.

The solidification dynamics and the resultant microstructural development during processing are examined in an effort to establish a processing/microstructure relationship. Existing models in the literature developed for splat cooling have been

extended and applied to examine the rapid-solidification process during plasma spraying. Microstructural features of the splats that are produced by individual impinging droplets are examined by scanning and transmission electron microscopy. The relation of dimensions and morphologies of these individual splats to the consolidated deposit microstructure is considered. In addition, distinguishing features in the solidification and microstructural development between air plasma spraying and vacuum plasma spraying (VPS) are explored. For instance, during VPS the rapidly solidified deposit is exposed to short-duration, self-annealing effects that can yield dense, fully recrystallized, ultrafine-grained microstructures. This has implications on the physical and mechanical properties of the deposit.

9. Numerical and Experimental Study of Nanostructured WC/Co Coating in the HVOF System

S. Eidelman, Science Applications International Corporation, VA, USA,
eidelman@apo.saic.com

Compared to conventional materials, the use of nanostructured materials can lead to improved coating quality and performance. This can significantly impact many defense and civilian technologies in terms of environmental compliance (e.g., hard-chrome replacement) and wear reduction, and lead to service-free operation of existing and future systems. Thermal spray processing offers a high-rate deposition method for nanopowder coating that can provide conditions required for sintering high-density nanostructured materials and forming high-quality coatings. However, the deposition regimes for nanopowders can be significantly different from regimes established for micron-sized materials.

A three-dimensional simulation capability was employed to analyze the thermal spray deposition of nanoscale WC/Co. Results from the numerical analysis were used to predict deposition conditions, which were then applied in practical deposition experiments. Using a high-speed optical pyrometer and PDA technique, particle size, velocity, and temperatures were measured and compared with numerical predictions. WC/Co nanoscale coatings were produced under different conditions, and their characteristics evaluated.

10. Diagnostics and Modeling of Nanostructured Thin-Film Synthesis in Low-Pressure Flames

N.G. Glumac, Y.-J. Chen, and B. Kear, College of Engineering, Rutgers University, Piscataway, NJ, USA, glumac@jove.rutgers.edu, and G. Skandan, Nanopowder Enterprises Inc., a Division of SMI, Piscataway, NJ, USA

While difficulties with spraying nonagglomerated nanopowder feedstocks have been reported under common thermal spray conditions, nanostructured thin films are readily produced at

high rates from 5 to 20 nm particles by low-pressure flame deposition (LPFD) methods (Ref 1, 2). In LPFD, a substrate on which a coating is desired is placed below a flat-flame burner, through

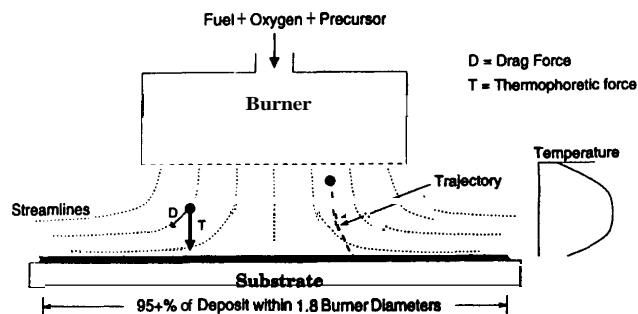


Fig. 6 Overview of the low-pressure flame synthesis (LPFS) process. The strong thermophoretic force in this environment ensures a localized and highly uniform nanostructured film.

which a mixture of fuel, oxygen, and precursor species passes. The entire assembly is placed in a chamber and maintained at reduced pressure. Nanoparticles condense in the gas phase (Ref 3) above the substrate, and the hot particles impinge upon the substrate and form a film. Reactor conditions can be varied such that the deposit is a dense (e.g., for protective coatings) or a porous film, with a controllable degree of porosity (e.g., for thermal barrier coatings) (Ref 4).

The conversion efficiency is extremely high, typically greater than 90%. That is, more than 90% of the metal atoms delivered to the system in the precursor are deposited in the film. Furthermore, the film deposition process is highly localized, with more than 95% of the deposition occurring within a circle of 1.8 times the burner radius. This result implies that the particles, despite their small size, do not follow the flow streamlines, which rapidly diverge at the substrate, as shown in Fig. 6. Calculations of particle trajectories suggest that the thermophoretic force in the region where streamlines diverge is as much as two orders of magnitude larger than the drag force, which scales with density, and is thus much reduced in these environments. The low pressure, coupled with the low momentum of the particles (speeds of <10 m/s) and the sharp temperature gradient in the flames, create an environment in which particles condensed at any radial location in the flame have similar trajectories toward

the substrate, leading to a high degree of uniformity in deposition rate and film quality.

Several diagnostic and modeling tools have been applied to the LPFD environment to understand the fundamental processes involved (Ref 5). Laser-induced fluorescence (LIF) of OH radicals has verified that the flame zone beneath the burner is radially uniform in OH concentration and temperature out to nearly the burner rim. In addition, LIF has been used to determine axial temperature and OH profiles that agree well with the predictions of a one-dimensional flame model using complex chemistry. These results suggest that the time/temperature history of the flow, which is critical in determining particle growth and agglomeration behavior, can be accurately calculated using conventional flame codes.

For particles, laser light scattering and thermophoretic probe sampling and flame emission spectroscopy have been applied to infer information about precursor decomposition rates, particle sizes, and particle number densities. Precursor decomposition occurs within the first quarter of the gap region between the burner and substrate. Particles of roughly 5 nm in diameter begin to appear at the one-quarter point, but do not increase significantly in size until the final quarter of the flame in which the mean particle diameter increases by a factor of 3 to 4.

References

1. Y.-J. Chen, N.G. Glumac, G. Skandan, and B. Kear, Scalable High-Rate Production of Non-agglomerated Nanopowders in Low Pressure Flames, *Mater: Lett.*, in press
2. Y. Chen, N. Glumac, B.H. Kear, and G. Skandan, High Rate Synthesis of Nanophase Materials, *Nanostructured Mater.*, Vol 9 (No. 1), 1997, p 101-104
3. D. Lindackers, M.G.D. Strecker, and P. Roth, Particle Formation Behavior in H_2/O_2 Low Pressure Flames Doped with SiH_4 and $TiCl_4$, *Nanostructured Mater.*, Vol 14 (No. 5), 1984, p 545-550
4. G. Skandan, N.G. Glumac, Y.-J. Chen, F.C. Cosandey, E. Heims, and B. Kear, Low Pressure Flame Deposition of Nanostructured Oxide Films and Coatings *J. Am. Ceram. Soc.*, in press
5. N.G. Glumac, Y.-J. Chen, and G. Skandan, Diagnostics and Modeling of Nanopowder Synthesis in Low Pressure Flames, *J. Mater. Res.*, in press

11. Characterization of Materials on the Nanoscale

M. Ruhle, Max-Planck-Institut für Metallforschung, Stuttgart, Germany

Nanostructured materials are materials where the length scale in at least one dimension ranges in the nanometer scale. The materials consist either of layered structured films (1-D nanoscale material), rodlike structures (2-D), or fine grained materials (3-D). The microstructure of the materials needs to be analyzed, and it is a priority to identify the different phases of the materials. The most adequate technique for phase identification is energy filtered transmission electron microscopy (EPTM). A quantitative evaluation of strains in the different constituents can be performed by convergent beam electron diffraction (CBED).

Most important is, however, the analysis of the structure and composition of internal interfaces because these defects often control the properties of the materials. In contrast to the studies of external interfaces (surfaces), there exists only a very limited number of experimental techniques for characterization of the internal interfaces. X-ray scattering experiments and transmission electron microscopy are the most important ones.

Advanced TEM techniques can be applied for the analysis of internal interfaces. Quantitative high-resolution TEM allows quantitative determination of the columns of atoms adjacent to

the interface. Analytical electron microscopy (AEM) enables determination of the composition of the interfaces with high-spatial resolution and an excellent limit of detectability. From

detailed electron energy loss spectroscopy (**EELS**) studies, information on electronic bonding, coordination number, and distances to neighboring atoms can be retrieved.

12. Cryogenic Heat Capacity Measurement and TPD Evaluation Methods on Ceramic Surfaces and Interfaces

*K. Ishizaki, Nagaoka University of Technology, Nagaoka, Japan,
ishizaki@mech.nagaokaut.ac.jp*

New surface and interface analysis techniques for ceramic powders and bulk materials have been developed. These have been applied to obtain qualitative and quantitative information on ceramic powder surfaces and grain boundaries.

The cryogenic heat capacity measurements based on Debye's T^3 law have successfully achieved accurate quantitative analysis for glassy and crystalline phases. The quantitative measurement of crystalline and amorphous grain boundary phases of silicon nitride sintered at various conditions has been studied. This technique has also been applied to evaluate alumina powder surfaces. It has measured the excess specific heat due to the specific surface, which is greater than that predicted

by Debye's law. The excess specific heat is governed by the atomic disorder on the surface, and comparisons to sintered porous samples show that the as-received powder has higher entropy than the sintered body.

The temperature programmed desorption (TPD) technique is a surface analysis technique that provides information on surface groups as well as the composition of the surface layer. This method has been applied to evaluate silicon nitride (Si_3N_4) powders. The desorption of adsorbates, desorption with recombination of surface groups, and decomposition and vaporization of the powder surfaces exhibit new relationships.

13. Effects of Production Processes on Si_3N_4 Powder Surfaces Characterized by TPD

T. Nakamatsu and K. Ishizaki, Nagaoka University of Technology, Nagaoka, Japan, ishizaki@mech.nagaokaut.ac.jp. Saito, Basic Research Center, INAX Corporation, Japan, and C. Ishizaki, Si-nano Technology Corporation, Nagaoka, Japan

Plasma spray processing is a simple and economic process to produce nanomaterial powders whose characteristics are governed by their surfaces due to their high specific surface area. Nitride ceramics are especially inevitably covered with oxides, which govern manufacturing efficiency and properties of the final products, for example, mixing behavior with additives, fluidity, sintering behavior, and properties of sintered materials. Silicon nitride (Si_3N_4), the most common structural ceramic material, exhibits a complex surface that consists of SiOH , SiNH_2 , Si_2NH , Si_2O , and/or SiH groups. The surfaces of Si_3N_4 powders were characterized by an ultrahigh vacuum temperature programmed desorption (TPD) technique. This is a nondestructive and sensitive surface analysis method that detects the desorbed gases generated by reactions between the surface groups.

Three types of commercial Si_3N_4 powders produced by different processes were investigated, that is, powders produced by (1) the silicon diimide precipitation process, (2) the carbother-

mal reduction process, and (3) the direct nitridation process of silicon (referred as powders A, B, and C, respectively). Liquid NH_3 was used as the nitridation medium for powder A while nitrogen gas was used for the other powders. Powder B was heat treated in air, and powder C was crushed and washed in acid and water. About 15 mg of powder sample was initially placed in a chamber preevacuated to 10^{-5} Pa, transferred into an ultrahigh vacuum chamber under 10^{-6} Pa, and heated up to 1450 °C at a constant heating rate of 20 K/min. During heating of the samples, the partial pressures of desorbed gases that are generated by the reactions and desorbed from powder surfaces are measured by a quadrupole mass spectrometer and the sample temperature and partial pressures of the desorbed gases recorded. Partial pressures of major desorbed species, H_2 , NH_3 , H_2O , and N_2 in the temperature range 40 to 1300 °C are calculated with their cracking patterns and relative sensitivity of the mass spectrometer, and normalized into desorption rates, R_d , the number

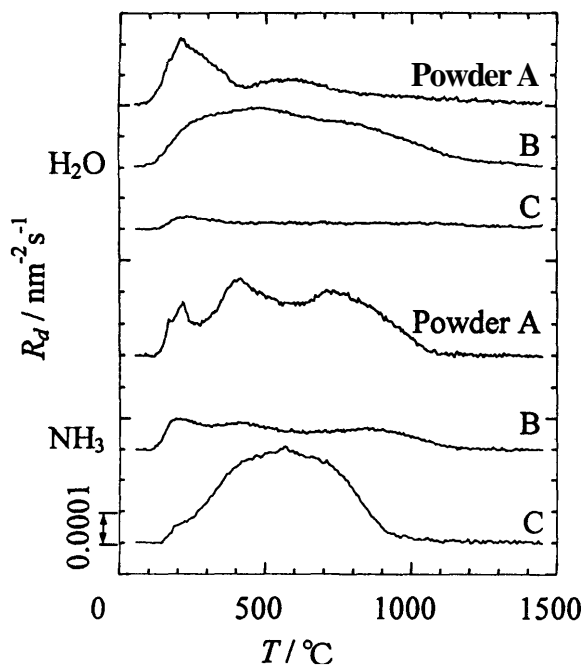


Fig. 7 Comparisons of H₂O and NH₃ TPD spectra normalized by specific surface area

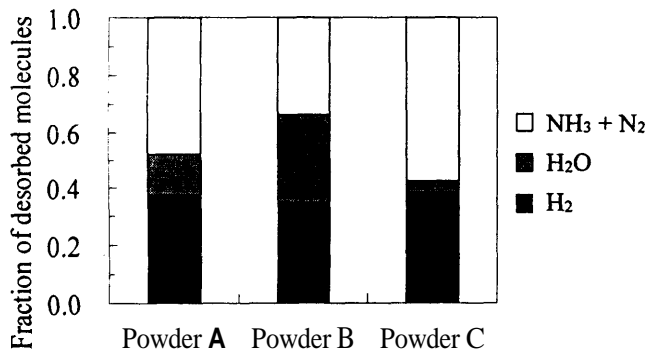


Fig. 8 Quantification of desorbed molecules characterize the Si₃N₄ powder surfaces in H₂O desorption as oxygen-related groups and NH₃ and N₂ as nitrogen-related surface groups

of desorbed molecules per unit time and unit area. The comparisons of processed H₂O and NH₃ TPD spectra between the Si₃N₄ powders are shown in Fig. 7. The quantification of desorbed

molecules by integration of TPD spectra as shown in Fig. 8 can characterize the raw Si₃N₄ powder surface states in H₂O desorption as oxygen-related surface groups and NH₃ and N₂ desorption as nitrogen-related surface groups.

Increase of the oxygen content by heat treatment in air and decrease by aqueous washing with respect to the surface amorphous layer thickness of Si₃N₄ powder has been studied by Yanai et al. (see Selected References below). Considering production methods and desorbed molecular fraction, powder B has the highest oxygen-related fraction that may be the result of oxidation by the final heat treatment in air. The oxidized surface can easily react with humidity in a storage condition to form -OH groups. The highest nitrogen-related fraction of powder C and the acid and aqueous washings decrease -OH and increase =NH/-NH₂ groups.

Selected References

- G. Busca, V. Lorenzelli, M.I. Baraton, P. Quintard, and R. Marchand, FTIR Characterization of Silicon Nitride Si₃N₄ and Silicon Oxynitride Si₂N₂O Surfaces, *J. Molec. Struct.*, Vol 143, 1986, p 525-528
- M. Kawamoto, C. Ishizaki, and K. Ishizaki, Fluidity-Increasing Behavior of Silicon Nitride Powder by Aqueous Washing, *Mate.: Sci. Lett.*, Vol 10, 1991, p 279-281
- M. Kawamoto, K. Ishizaki, and C. Ishizaki, Temperature Programmed Desorption as a Surface Characterization Method of Ceramic Powder, *Handbook on Characterization Techniques for the Solid-Solution Interfaces*, J.H. Adair, J.A. Casey, and S. Venigalla, Ed., American Ceramic Society, 1993, p 283-292
- G. Ramis, G. Busca, V. Lorenzelli, M. Baraton, T. Merle-Mejean, and P. Quintard, FT-IR Characterization of High Surface Area Silicon Nitride and Carbide, *Surf. Int. Ceram. Mater.*, Dufour et al., Ed., Kluwers Academic Publishers, 1989, p 173-184
- N. Saito, C. Ishizaki, and K. Ishizaki, Temperature Programmed Desorption (TPD) Evaluation of Aluminum Nitride Powder Surfaces Produced by Different Manufacturing Processes, *J. Ceram. Soc. Jpn.*, Int. Ed., Vol 102 (No. 3), 1994
- T. Yanai and K. Ishizaki, Effect of Surface Oxidation of Si₃N₄ Powder on Mechanical Properties and Microstructure of Sintered Products, *J. Jpn. Inst. Met.*, Vol 59 (No. 9), 1995, p 984-989
- T. Yanai and K. Ishizaki, Influence of Oxygen Content on the Mechanical Properties of In-Situ Formed Si₃N₄-SiC Nanocomposites Prepared by Carbon Coating Method, *J. Ceram. Soc. Jpn.*, Int. Ed., Vol 103 (No. 7), 1995, p 734-736
- T. Yanai and K. Ishizaki, Influence of Oxygen Impurity Content on the Surface Oxidized Layer Thickness of Si₃N₄ Powders, *J. Ceram. Soc. Jpn.*, Int. Ed., Vol 103 (No. 7), 1995, p 746-748

14. Synthesis of Titanium Aluminide Base Composites by Reactive Thermal Spraying

K. Murakami, T. Kawanaka, Y. Miyamoto, and H. Nakajima, Osaka University, Osaka, Japan, murakami@sanken.osaka-u.ac.jp, and T. Kujim, College of Industrial Technology, Amagasaki, Japan, kujime@cit.sangitan.ac.jp

Titanium aluminide base composites with fine ceramic dispersoids were produced by reactive thermal spraying of two

types of composite powders, Fig. 9. The cores of the first and second types of powders are titanium aluminide and tita-



Fig. 9 Scanning electron micrographs of sprayed deposits containing 2.0 wt% B. (a) As-sprayed deposit. (b) Deposit heat treated at 1173 K for 2 h

nium/aluminum composite powders, respectively, and both are coated with elemental boron. The main constituents of the as-sprayed deposits are Ti_3Al (α_2) phase and $TiAl$ (γ) phase, which are supersaturated with boron resulting from the high cooling rate during solidification of the melts. Heat treatment of the deposits at and above 1023 K results in precipitation of extremely fine TiB_2 particles. Despite the precipitation, the hardness of the deposit decreases on heat treatment, which is explained in terms of matrix softening due to the increase in the fraction of the γ

phase of low hardness and to the elimination of the rapid solidification structures. The hardness of the heat treated deposits, however, is higher than that of the titanium aluminide having the same composition as that of the matrix of the composites. Coarsening of the TiB_2 particles is not significant until temperatures of 1473 K. The heat treated deposits produced from the second composite powder contain Ti_2AlC particles as well as TiB_2 particles, the carbon coming from methanol used as the process control agent for the fabrication of the titanium/aluminum core powder.

15. Novel Engineering Coatings with Nanocrystalline and Nanocomposite Structures by HVOF Spraying

D.A. Stewart, A.H. Dent, S.J. Harris, A.J. Horlock, D.G. McCartney, and P.H. Shipway, Nottingham University, Nottingham, England, emxdas Bemnl.nott.ac.uk

The application of a surface coating to a bulk material can extend the lifespan of a component considerably. The use of feedstock powders that produce nanoscale microstructural features in deposits can enable coatings of higher strength, hardness, and corrosion resistance to be deposited. HVOF thermal spraying was used to deposit Ni-base Metco 700 and WC-Co-base Nanocarb. The effect of spray variables such as fuel gas type (propylene/hydrogen), fuel-to-oxygen ratio, spray distance, powder feed rate, and substrate cooling on coating characteristics were investigated. The coatings were evaluated in terms of microhardness, wear, and corrosion resistance. This evaluation was then related to the microstructural features that result from the spray process such as decarburization, oxidation, and metastable phase formation as characterized through the use of SEM, plan-view, and cross-sectional TEM and XRD.

XRD and TEM characterization of the as-sprayed WC-Co nanocomposite coating revealed varying degrees of decomposition of the original (50 to 200 nm) WC. Blocky unreacted carbides (Fig. 10) as well as rounded reacted WC with 30 to 100 nm

thick shells of W_2C were observed within an amorphous matrix. Furthermore, the high surface area to volume ratio of the nanocomposite powder also resulted in the presence of W_2C with a surface shell of W, demonstrating a complete decomposition of some original carbides.

A range of inert atmosphere heat treatments performed on the nanocomposite coatings revealed a partial recrystallization of the amorphous matrix to an η carbide (Co_6W_6C) at $T > 700^\circ C$. The abrasive wear characteristics of the as-sprayed and heat treated WC-Co nanocomposite coatings were also investigated. Heat treatment improved the wear performance of these nanocomposite coatings, thereby corroborating other work in this field (Ref 1-3). Future work lies in optimizing the process parameters to limit the amount of decomposition in the coating.

Spray trials of the Metco 700 alloy were conducted using a matrix of experiments based upon the Taguchi method to optimize hardness, wear, and corrosion resistance. Significant variations were noted in the performance of Metco 700 coatings depending on spray conditions. XRD and TEM investigations of

the coatings revealed a large proportion of nanocrystalline/amorphous material within the deposits (Fig. 11) as well as the usual cellular microstructures observed in plasma sprayed coatings of this alloy (Ref 4). Increases in the concentration of the nanocrystalline/amorphous phases were directly related to enhancements in hardness (550 to 700 HV) and abrasive wear resistance. Oxidation of the powder during spraying was observed as columnar grained $\alpha\text{Cr}_2\text{O}_3$ stringers and globular NiCr_2O_4 spinels within coatings.

Potentiodynamic testing of the Metco 700 coatings in 0.5 M H_2SO_4 (Ref 5) showed greater resistance to corrosion of the deposits compared to as-sprayed Inconel 625 coatings. Optimization of the corrosion resistance of the Metco coatings appeared to be directly related to a reduction in the proportion of oxide (as measured by quantitative EDX and XRD peak area measurements) within the deposits.

The current development of alloys with optimized compositions based upon the Ni-Cr-Mo-B system containing greatly increased nanocrystalline/amorphous concentrations has shown improvement in properties due to processing to achieve fine-scale microstructures. Significantly better resistance to both abrasive wear and potentiodynamic corrosion compared to HVOF-sprayed Metco 700 and Inconel 625 coatings have been measured as well as hardnesses of ~800 to 950 HV.

References

1. C.J. Li, A. Ohmori, and Y. Harada, Formation of an Amorphous Phase in Thermally Sprayed WC-Co, *J. Therm. Spray Technol.*, Vol15 (No. 1), 1996, p 69-73
2. J. Nerz, B. Kusher, and A. Rotolico, Microstructural Evaluation of Tungsten Carbide-Cobalt Coatings, *J. Them. Spray Technol.*, Vol 1 (No. 2), 1992, p 147-152
3. D.A. Stewart, P.H. Shipway, and D.G. McCartney, Influence of Heat Treatment on the Abrasive Wear Behaviour of HVOF Sprayed WC-Co Coatings, *Surf. Coat. Technol.*, in press
4. S. Sampath, R.A. Neiser, H. Herman, J.P. Kirkland, and W.T. Elam, A Structural Investigation of a Plasma Sprayed Ni-Cr Based Alloy Coating, *J. Mater. Res.*, Vol18 (No. 1), 1993, p 78-86
5. "Standard Reference Test Method for Making Potentiostatic and Potentiodynamic Anodic Polarization Measurements," G5-94, *Annual Book of ASTM Standards*, American Society for Testing and Materials, 1994, p 48-58

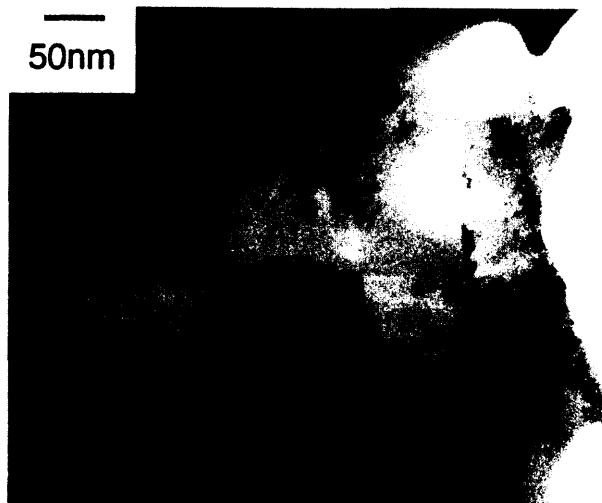


Fig. 10 Blocky unreacted carbides with more rounded reacted WC with 30 to 100 nm thick shells of W_2C within an amorphous matrix

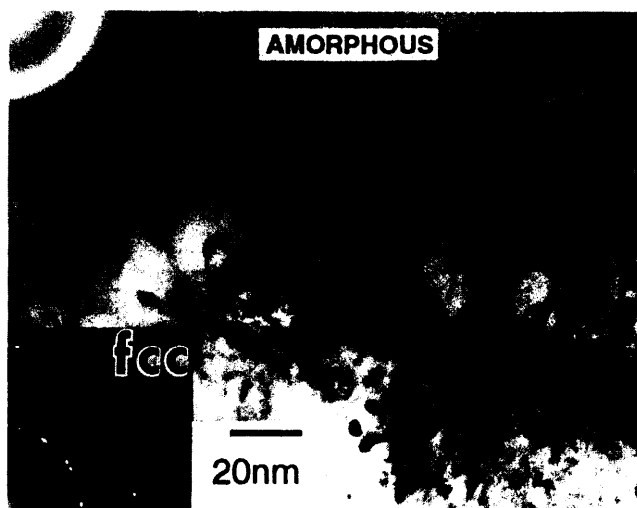


Fig. 11 XRD and TEM of the coatings show a large proportion of nanocrystalline/amorphous material within the deposits as well as cellular microstructures

16. Plasma Spray Synthesis of Nanozirconia Powder

'C.C. Berndt, T. Chraska, and A.H. King, SUNY Stony Brook, NY, USA,
cberndt@ccmail.sunysb.edu, and J. Karthikeyan, Heany Industries Inc., NY, USA

Nanomaterials have many unique properties and have large industrial potential. In particular, because nanozirconia can retain the metastable, transformable tetragonal phase, it can be used to produce transformation-toughened zirconia bulk forms (Ref 1). Nanozirconia powders can be produced by a variety of techniques including the plasma spray synthesis (PSS) process (Ref 2-4) developed at Stony Brook. In the PSS process (Ref 2)

(Fig. 12), a liquid precursor solution is atomized, and this aerosol is injected into a high-temperature plasma flame. Nanoparticles, synthesized by plasma-droplet interactions, are collected as powder on an electrostatic precipitator (Fig. 13).

Preliminary experiments (Ref 2) showed that many process parameters influence the process characteristics and properties of the synthesized powders. Hence a Taguchi style, two-level

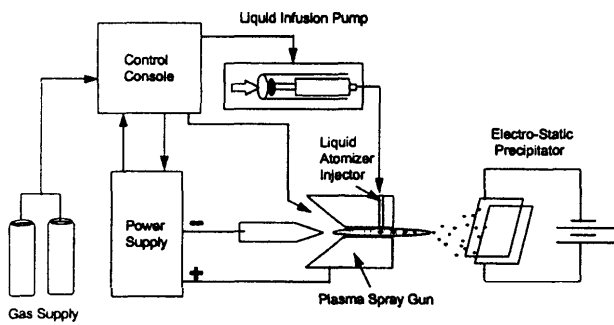


Fig. 12 The thermal spraying of liquids process where a liquid precursor is atomized and injected into the high-temperature plasma flame. The plasma synthesized particles are collected as a deposit on a substrate or as powder on an electrostatic precipitator. The atomized droplet enters the high-temperature flame and is accelerated toward the collecting surface, and various phenomena occur.

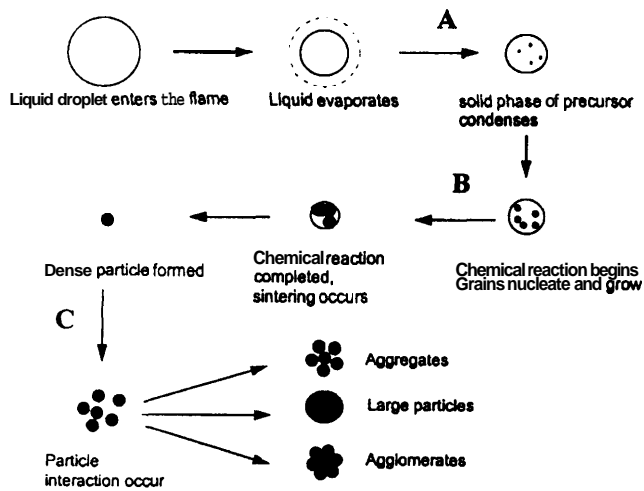


Fig. 13 The atomized droplet enters the high-temperature flame and is accelerated toward the collecting surface, and various phenomena occur: (1) The first step is the *evaporation* of the solvent. (2) The next stage is *condensation* of the precursor materials and *initiation of chemical reactions*. (3) *Nucleation and growth* of the grains must then occur; followed by formation of dense particles. (4) *Interactions* among these highly active particles lead to the formation of either large particles/crystals, agglomerates, or aggregates.

four-variable, design of experiment was performed to map the effect of process variables. A modified plasma spray gun was used to synthesis nanomaterials, and process parameters such as feedstock concentration, liquid feed rate, stand-off distance, and the electric field of the electrostatic precipitator were systematically studied. The process characteristics were established by measuring the deposition efficiency (DE) and deposition rate of the synthesized powders. Characteristics of the powders, such as the particle size distribution and phase composition, were measured using XRD, TEM, and SANS.

The results of this study can be summarized as follows:

- Nanozirconia powders with 3 to 80 nm size particles can be produced by the PSS process, for example see Fig. 14.

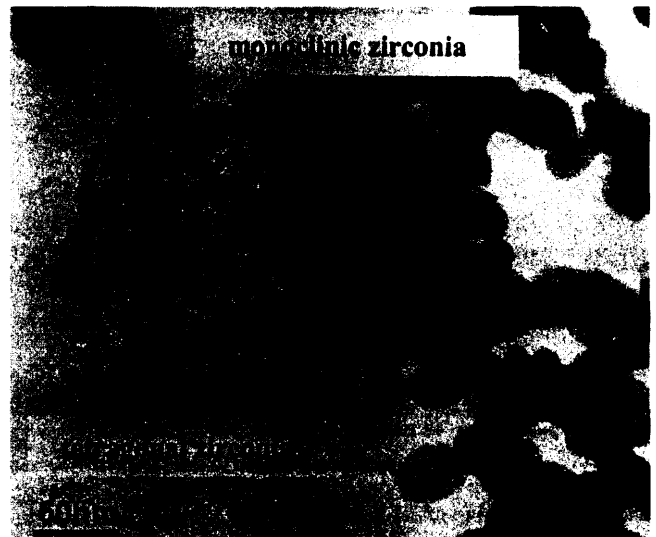


Fig. 14 TEM inspection of the particles reveals that they adopt one of two distinct crystal structures, depending on their size. The smallest particles have the tetragonal structure, while larger ones are monoclinic.

- Nanopowder could be collected with a deposition efficiency (DE) of 3 to 15%, at a collection rate of about 5 to 100 mg/min. (Note that this study was not intended to optimize DE.)
- The presence of an electric field in the electrostatic precipitator strongly enhances the DE and deposition rate of the process, but does not have significant effect on the particle size distribution.
- The distance between the plasma gun and the collecting surface does not have significant influence on either process characteristics or properties of the nanomaterials.
- Increasing the feedstock concentration and liquid feed rate result in an increased deposition rate, but the average particle size distribution exhibits a slight increase.
- The DE of the process does not depend on the concentration of the precursor feedstock, but slightly decreases with an increase in liquid feed rate.

References

1. C.A. Anderson and P.K. Gupta, *Advances in Ceramics, Vol 3, Science and Technology of Zirconia*, A.H. Heuer and L.W. Hobbs. Ed.. The American Ceramic Society, 1981, p 184-201
2. J. Karthikeyan, C.C. Berndt, J. Tikkanen, S. Reddy, and H. Herman. Plasma Spray Synthesis of Nanomaterial Powders and Deposits. *Mater. Sci. Eng. A*, Vol 238 (No. 2), 1997, p 275-286
3. G. Skandan, Processing of Nanostructured Zirconia Ceramics, *Nanostructured Mater.*, Vol 5 (No. 2), 1995, p 111-126
4. J. Karthikeyan, C.C. Berndt, J. Tikkanen, J.Y. Wang, A.H. King, and H. Herman, Preparation of Nanophase Materials by Thermal Spray Processing of Liquid Precursors, *Nanostructured Mater.*, Vol 9, 1997, p 137-140

17. Diagnostic and Modeling Tools for Optimizing Thermal Spray Processes

R.A. Neiser and M.F. Smith, Sandia National Labs, Albuquerque, NM, USA, ranneise@sandia.gov

Noninvasive diagnostic techniques combined with numerical and analytical models greatly enhance understanding of thermal spray processes. These tools provide important means for obtaining tailored properties and microstructures in the sprayed deposits. Work between Sandia National Labs and General Motors Corporation under a cooperative research and development agreement (CRADA) studied a HVOF process for depositing wear-resistant cylinder bore coatings in aluminum automobile engines. This work describes the methods that were employed in optimizing the HVOF process and include analytical, numerical, and statistical modeling; noninvasive particle and flame diagnostics; and new process control and data logging algorithms. These methods would also be useful in optimizing thermal spray processes for nanoscale deposits.

In addition, information regarding technology that has emerged from the former Soviet Union, cold-gas spray processing (CSP), is investigated. CSP may have great potential for pro-

ducing dense, well-adhered deposits of nanoscale wear- and corrosion-resistant materials. CSP uses a supersonic jet of compressed air to accelerate small powder particles to ~300 to 1240 m/s and is cost effective. Above a critical minimum velocity, the high kinetic energy of the spray particles becomes sufficient to cause them to flow and consolidate upon impacting the target surface, even though the particles arrive at the surface far below their melting or softening temperatures. Because it is not combustion-based, CSP does not degrade thermally sensitive coating materials either through oxidation or other in-flight chemical reactions. CSP may be an excellent candidate process for producing nanoscale materials because of the low processing temperature, the minimal extent of oxidation, the low porosity of the deposits, and the high deposition efficiency. A cold-spray facility is currently being brought on-line at Sandia, and its capability for producing high-quality nanoscale materials will be examined.

18. VPS Nanophase Alumina-Zirconia for Thermal Barrier Coating Applications

V. Provenzano and L. Kuriharai, Naval Research Laboratory, Washington, DC, USA, provenzanoQanvii.nrl.navy.mil, G.E. Kim, PERMA a Division of PyroGenesis Inc., Quebec, Canada, and E.V. Barrera, Rice University, TX, USA

Nanoscale alumina-zirconia coatings have been deposited by vacuum plasma spraying (VPS) onto metallic substrates. The aims of this effort were: (1) to demonstrate the feasibility of using VPS technology to deposit **nanoscale** coatings for high-temperature applications, (2) to show that a nanocomposite approach allows the retention of the nanoscale microstructure at high temperatures, and (3) to tailor and optimize the coating properties by varying the deposition parameters and composition.

This work is based on earlier results on **nanocomposite** alumina-zirconia samples where colloidal suspensions were consolidated by high-temperature **sintering**. The earlier study

demonstrated the ability of alumina to stabilize the high-temperature tetragonal phase in zirconia via a nanocomposite approach. This nanocomposite approach relies on the immiscibility between alumina and zirconia to suppress grain growth and, thus, retain both the nanoscale microstructure and phase stability at high temperatures. There are advantages of using alumina-stabilized nanoscale zirconia over conventional yttria-stabilized TBC coatings. Vacuum thermal spraying can be an attractive and versatile technology for depositing nanoscale coatings with improved properties for a variety of naval applications.

19. Microstructure and Properties of Plasma Sprayed Nanoscale Tungsten Carbide-Cobalt Coatings

M. Scholl, M. Becker, and D. Atteridge, Oregon Graduate Institute of Science and Technology, OR, USA, milts@mse.ogi.edu

A -120 + 10 μm WC-15Co powder consisting of nanoscale WC in a cobalt matrix was sprayed using a high-energy plasma

system. For comparison, a conventional -45 + 11 μm WC-12Co powder was sprayed under similar conditions. The plasma sys-

tem differs from conventional systems by working at lower currents (up to 500 A) and high voltages (up to 500 V). The plasma system was operated at a nominal 150 kW and over a range of gas flows, which yielded plasma velocities from subsonic to supersonic. Nitrogen primary plasma gas flows ranged from 200 to 300 slpm and hydrogen secondary gas flow ranged from 0 to 100 slpm. Additionally, a tertiary hydrocarbon gas was added in some tests. The resulting coatings were sectioned and examined metallographically and microhardness tests performed. Several coatings and the starting powder were examined using x-ray diffraction. As well, several coatings were tested under three-body abrasion in an ASTM G-65 Dry-Sand-Rubber-Wheel test with silica sand. The results of the abrasion tests were compared to other coating materials and to cast abrasion-resistant materials.

The microstructure of the nanoscale coating was resolvable only at high magnifications in a scanning electron microscope, showing carbides about 100 nm in size. In contrast, the carbides in the conventional WC-12Co material were 5 to 10 μm . With both types of starting powders, the coating porosity was very low, especially in the nanoscale WC-15Co coatings where microscopic porosity was not observable under optical microscopy. However, cracking was observed in the conventional WC-Co but not in the nanoscale WC-Co. X-ray diffraction of the as-received powder showed distinct WC and Co peaks while

in the coating WC, W, and W_2C peaks were observed along with several unidentified peaks. Broadening of unidentified peaks was observed instead of cobalt peaks, suggesting amorphous or microcrystalline grain sizes or nonstoichiometric compounds. Amorphous and microcrystalline regions in the cobalt matrix were identified by transmission electron microscopy. Knoop hardnesses ranged from 850 to 1100 HK_{500} depending on the operating parameters for the nanoscale WC-Co. The hardness of the conventional WC-Co was about 920 HK_{500} .

The nanoscale coatings showed little variation in microstructure and hardness despite the wide variation in deposition parameters. Additions of a tertiary hydrocarbon gas to the plasma jet increased the hardness of the nanoscale coatings by about 10%, but had little effect on the conventional WC-12Co coatings. The abrasive wear resistance of the nanoscale WC-15Co coatings was equivalent to the best results of the other conventional WC-12Co coatings tested, as well as to $\text{Cr}_3\text{C}_2\text{-25NiCr}$ coatings. There was a much greater scatter in the wear tests of the conventional WC-Co compared to the tests on the nanoscale WC-Co. In comparison to cast high-chromium irons, a 25Cr white iron and a 20Cr-2Mo-1.5Ni-1.5Cu white iron, the nanoscale WC-Co coatings exhibited similar wear resistance. Additionally, despite being deposited over extremes of deposition parameters, the wear resistance of the nanoscale WC-Co coatings varied only slightly.

20. Particulate Nanoreinforced Polymer Composites: Processing and Properties

*E. Petrovicova, R.W. Smith, and R. Knight, Drexel University, PA, USA,
sg9574m2@dunxl.ocs.drexel.edu and L.S. Schadler, Rensselaer Polytechnic Institute, NY, USA*

Nanoreinforced polymer composites have recently attracted considerable attention because they exhibit unique mechanical properties compared to their conventional microcomposite counterparts. Dramatic improvements in modulus, wear and scratch resistance, and barrier properties have been observed following the addition of nanoscale ceramic particles to polymer matrices. The technical challenge in processing these composites is to achieve dispersion of the ceramic phase within the polymer matrix, which requires aids such as a low-melt viscosity polymer or solvents.

The HVOF combustion spray process is a powerful coating technique that allows solventless processing of ceramic-reinforced polymers and does not require melt processing. A key advantage of HVOF over other coating processes is that the deposition of nanoreinforced composites is not limited by the size of the part and coatings can be readily applied in the field. This is a key factor because these materials have significant potential applications in industry as corrosion barriers.

Results have shown that HVOF processing of nylon 11 composites reinforced with nanosized hydrophilic and/or hydrophobic silica and carbon black is feasible. The coatings exhibited 30

and 50% improvements in scratch and sliding wear resistance, respectively (Fig. 15). The measured increase in dynamic storage modulus of the composites was also much larger than predicted by the rule of mixtures, as shown in Fig. 16. Current research is focused on understanding the fundamental reinforcing mechanisms in thermally sprayed nanocomposite coatings and the effects of matrix/filler interactions on coating mechanical and barrier properties.

The influence of processing parameters and particulate surface chemistry (hydrophobic versus hydrophilic) on coating microstructure and filler distribution and dispersion have been studied. Improved distribution of the filler resulted in a 20% decrease in scratch depth and a 15% decrease in wear track area. A large inhomogeneity in the distribution of the filler resulted in coatings with clearly discernible "cell structures" consisting of large areas of unreinforced polymer matrix surrounded by agglomerates of filler, which adversely affected the scratch and wear performance of the coatings. Experiments showed that optimized HVOF spray parameters, promoting complete "in-flight" melting of the polymer powders, enabled these microstructural inhomogeneities to be virtually eliminated.

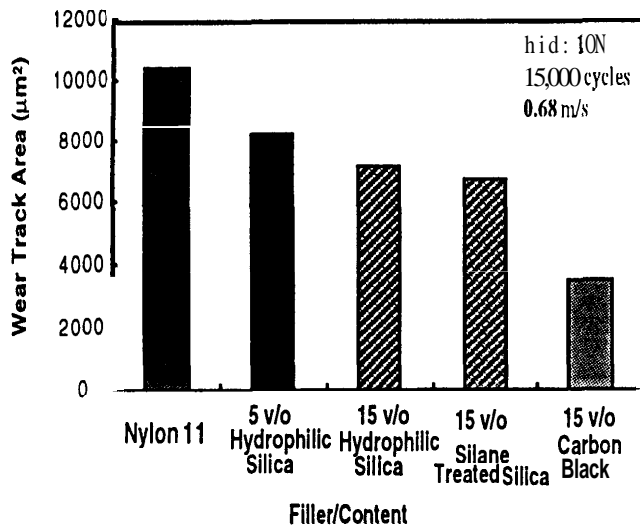


Fig. 15 Sliding wear test results for different type of fillers. Decrease in the wear track area measured after 15,000 cycles is shown.

All nanoreinforced coatings exhibited increased fractional crystallinity compared to pure nylon 11 coatings. A strong correlation was found between coating crystallinity and coating performance, and it was hypothesized that the filler particles served as nucleation sites, thus promoting crystallization. The increase in crystallinity depended on filler morphology and surface chemistry. Carbon black, for example, caused a larger increase in crystallinity than silica, and hydrophilic silica produced a larger increase in crystallinity than hydrophobic silica. It is unclear at this point if this was due to improved dispersion of the carbon black and hydrophilic fillers or whether this was due to changes in **matrix/filler** interactions. Changes in crystallinity alone cannot completely explain the observed differences in behavior of hydrophobic and/or hydrophilic silica and carbon black fillers. Clearly, filler surface chemistry affects both the dispersion of the particles and the functionality of the fillers as traditional load-bearing reinforcements.

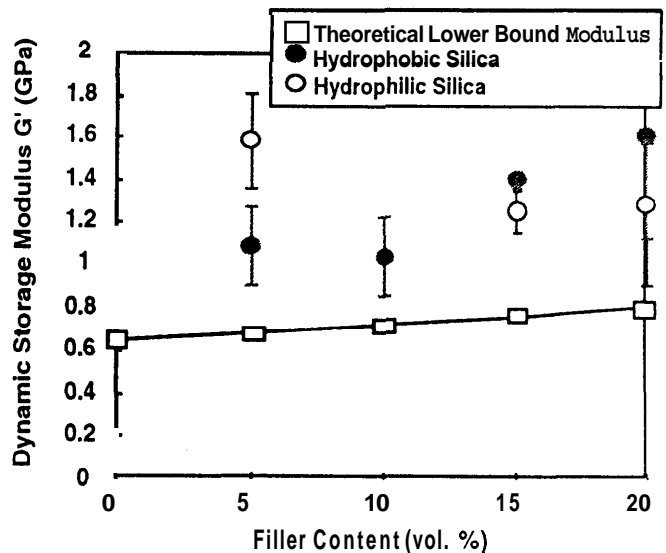


Fig. 16 Change in the dynamic storage modulus with increasing amount of the filler in the nanocomposites and comparison to calculated values for the lower-bound modulus prediction

Selected References

- E. Giannelis, A New Strategy for Synthesizing Polymer-Ceramic Nanocomposites, *JOM*, Vol 44 (No. 3), 1992, p 28-30
- R. Krishnamoorti, R.A. Vaia, and E.P. Giannelis, Structure and Dynamics of Polymer-Layered Silicate Nanocomposites, *Chem. Mater.*, Vol 7 (No. 9), 1996, p 1728-1734
- E. Petrovicova, L.S. Schadler, R. Knight, and R.W. Smith, Structure and Properties of HVOF Sprayed Ceramic/Polymer Nanocomposite Coatings, *Thermal Spray: A United Forum for Scientific and Technological Advances*, C.C. Berndt, Ed., ASM International, 1998
- L.S. Schadler, K.O. Laul, R.W. Smith, and E. Petrovicova, Microstructure and Mechanical Properties of Thermally Sprayed Silica/Nylon Nanocomposites, *J. Therm. Spray. Technol.*, Vol 6 (No. 4), 1997, p 475-485

21. Thermal Stability of Nanostructured Metal Alloys

J.C. Rawers, Albany Research Center, OR, USA, rawers@alrc.doe.gov

Nanostructured materials have enhanced properties that make them attractive for many industrial applications where the surface environment requires special attention. One means of producing nanostructured coatings is by thermal spraying of nanostructured powders. Although thermal spray processing has centered around the development of wear-resistant, nanostructured WC-Co coatings, of equal interest is the possibility of developing nanostructured metallic coatings. Nanometallic surfaces can offer unique combinations of properties such as high

strength and toughness, increased corrosion resistance, excellent wear properties, improved resistance to thermal fatigue, and so forth (Ref 1).

However, before nanostructured materials can be considered for commercial applications, two concerns must be addressed: (1) production of sufficient quantities of material for industrial applications and (2) retention of nanostructured properties during the coating process. The first concern is with the scaling up of production capabilities from laboratory to industrial de-



Fig. 17 Micrograph of mechanically alloyed Fe-2wt% Al thermally aged for 25 min at 900 °C. Milled particles are outlined with fine sub-micron grain bcc-iron; within the particles are nanograins of iron and a fine aluminum oxide precipitates. Several of the particles have little or no oxides present.

Table 2 Grain size (nm) of iron powder, mechanically processed iron powder, and iron powder processed with 2 wt% Al when subjected to elevated temperatures for extended periods of time

Composition	As received iron powder	Mechanically processed iron powder	Mechanically alloyed Fe-2wt% Al
As processed	100	8	5
700 °C, 25 min	190	30	18
800 °C, 25 min	410	85	20
900 °C, 25 min	>1000	130	40
1000 °C, 25 min	>>1000	140	120

mands. This problem has been addressed with the production of nanostructured materials by high-energy milling. For example, attritor milling can produce kilogram quantities of micrometer-sized particles with nanostructure grains (Ref 2-4).

The second concern is with the retention of the nanostructured properties from the milled powder being retained through a thermal technique (i.e., a high-temperature application). The thermal stability of the nanostructure is important because thermal spraying requires powders to be heated to temperatures near the melting point. Recent studies of nanostructured powders produced by mechanical alloying have shown that the thermal stability of these milled powders can be retained even when heated to elevated temperatures for extended times (Ref 3-5).

The processing characteristics of thermal spraying greatly enhance the probability of retaining milled nanostructure properties. The rapid heating and the short time at elevated tempera-

tures before the powders come into contact with a cold surface restricts the time for grain growth, for elemental diffusion, and for the formation and growth of second-phase precipitates. Also, the kinetic energy of the thermal spray process when particles impact against the substrate allows for formation of a relatively porous free coating without the necessity of melting the powder particles.

A particularly interesting metallic system for thermal spray application is the **bcc-Fe** alloys. Attrition milling of iron powders forms nanostructured micrometer-sized particles. When small quantities of alloying powder are milled with iron powder, the alloying powder tends to develop into a thin layer on the nanograin boundaries. If the particles are exposed to the open atmosphere, an oxide coating develops on the particle surface. When the particles are heated and consolidated, as occurs during the thermal spray application, the surface oxide layer reacts with the particle alloying element (aluminum, chromium, niobium) forming fine **nanoprecipitates** on the **bcc-Fe** nanograins that reduce grain growth (Fig. 17).

For iron alloys there is an additional grain refinement process, that is, the **bcc-Fe** ↔ **fcc-Fe** phase transition. When the powder is heated to 912 °C in the thermal spray gun and then during the subsequent rapid cooling stage when the powder is coated onto the cold metal surface, there is the **fcc-Fe** to **bcc-Fe** phase transition that acts as a grain-refinement process. Both alloying and phase transition can be effective in retaining the nanostructure properties (Table 2).

Thus, thermal spraying is a practical means of applying surface coatings of nanostructured metal powders while at the same time retaining the enhanced properties of nanostructured materials. Studies are currently underway to determine whether fine second-phase ceramic (carbides, nitrides, oxides) powders can be added either during the milling or to the milled powder during spraying to enhance the wear characteristics and the fracture toughness and to improve thermal fatigue properties of nanostructured coatings.

References

1. "Mechanically Alloyed and Nanocrystalline Materials," A. Reza Yavari, Ed., *Materials Science Forum*, Vol 179-181
2. J.C. Rawers, Study of Mechanically Alloyed Nanocrystalline Iron Powder, *J. Mater. Synthesis Process.*, Vol 3 (No. 1), 1995, p 69-79
3. J. Rawers and G. Korth, Microstructure of Attrition Ball-Milled and Explosively Compacted Iron Powder Alloys, *Nanostructured Mater.*, Vol 7 (No. 1/2), 1996, p 2S-4S
4. J. Rawers, G. Slavens, D. Govier, C. Dogan, and R. Doan, Microstructure and Tensile Properties of Compacted, Mechanically Alloyed, Nanocrystalline Fe-Al Powders, *Metall. Mater. Trans. A*, Vol 27A, 1996, p 3126
5. J. Rawers, G. Slavens, R. Krabbe, and J. Groza, Hot-Press Consolidation and Tensile Strength Characterization of Mechanically Alloyed Nanostructured Fe-Al and Fe-C Powder, *Nanostructured Mater.*, Vol 9, 1997, p 197-200

22. Mechanical Properties of Nanocrystalline Materials

C.C. Koch, North Carolina State University, NC, USA, carl_kock8ncsu.edu

A state-of-the-art interpretation of the mechanical properties of nanostructured materials concluded that the elastic moduli of nanocrystalline (nc) materials are unchanged from those of coarse-grained materials until very small grain sizes, <10 nm, are reached such that the atoms associated with grain boundaries and triple junctions become a significant fraction of the total (Ref 1). Nanocrystalline metals are very hard and strong, with hardness typically increasing as grain size decreases, that is, "Hall-Petch" behavior. The negative Hall-Petch behavior observed at the finest grain sizes in some experiments is in most cases due to changes in structure promoted by annealing for grain growth. The effect of grain size on hardening overwhelms solid-solution hardening for substitutional solid-solution nc alloys (Ref 2). Therefore, in some nc alloys an apparent solid-solution softening is observed that is really due to the influence of

the alloy addition on grain size, for example, increasing the grain size.

Nanocrystalline materials with small grain sizes (<25 nm) and at "low" temperatures (<0.5 melting temperature) exhibit little tensile ductility. This is shown in Fig. 18 where tensile elongation is plotted against grain size for a number of nc pure metals (e.g., Cu, Ag, Pd, Al) and alloys that in coarse-grained form have elongations of typically 30 to 60%. A large asymmetry in strength and especially ductility is seen between tensile and compressive testing. Enhanced superplastic behavior (lower temperature range, higher strain rates) is observed in nc materials above the "equicohesive" temperature, that is, where the fine-grain material is weaker than coarse-grain samples. However, no evidence has been reported for low temperature (<0.5 melting temperature) tensile superplasticity in fine-grained nc materials (Ref 3). Similarities are noted between deformation of nc and amorphous materials. The observation of shear bands, asymmetry between tensile and compressive behavior, and little or no work hardening are some common features (Ref 4). The deformation mechanisms for nc materials are not yet understood.

References

1. T.D. Shen, C.C. Koch, T.Y. Tsui, and G.M. Phatt, On the Elastic Moduli of Nanocrystalline Fe, Cu, Ni, and Cu-Ni Alloys Prepared by Mechanical Milling/Alloying, *J. Mater. Res.*, Vol 10, 1995, p 2892-2896
2. T.D. Shen and C.C. Koch, Formation, Solid Solution Hardening and Softening of Nanocrystalline Solid Solutions Prepared by Mechanical Attrition, *Acta Mater.*, Vol 44, 1996, p 753-761
3. M.J. Mayo, High and Low Temperature Superplasticity in Nanocrystalline Materials, *Nanostructured Mater.*, Vol 9, 1997, p 717-761
4. J.E. Carsley, R. Shaik, W.W. Milliga, and E.C. Aifantis, Mechanical Behavior of Bulk Nanostructured Fe/Cu Alloys, *Chemistry and Physics of Nanostructures*, E. Ma, B. Fultz, R. Schull, J. Morral, and P. Nash, Ed., TMS, 1997, p 183-192

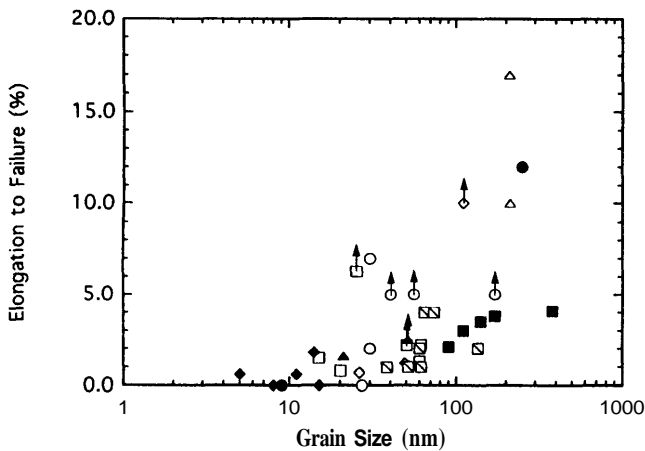


Fig. 18 Dependence of the ductility of nanocrystalline pure metals (e.g., Cu, Ag, Pd, Al) with respect to grain size

23. HVOF Processing of Nanostructured WC-Co Coatings and Their Properties

S. Usmani, S. Sampath, and H. Herman, SUNY at Stony Brook, NY, USA, susmani8ccmail.sunysb.edu

Sintered and thermal sprayed WC-Co are widely applied in industrial applications for wear control (Ref 1, 2). The commercially available WC-Co powders that are widely used in the thermal spray industry contain WC particles dispersed in a Co matrix with median WC sizes generally ranging from 1.5 to 7.5 μm (Ref 2). Recently, there has been interest in tribological ap-

plications of nanostructured WC particles dispersed in a Co matrix ($n\text{WC-Co}$) containing, typically, $n\text{WC}$ particles smaller than 0.1 μm .

It has been shown that thermal spraying of WC-Co leads to decomposition of the WC phase with subsequent dissolution of the W and C in the Co matrix to produce complex $\text{Co}_x\text{W}_y\text{C}$ (Ref



Fig. 19 Optical micrograph displaying a dense microstructure of the nWC-15%Co coating

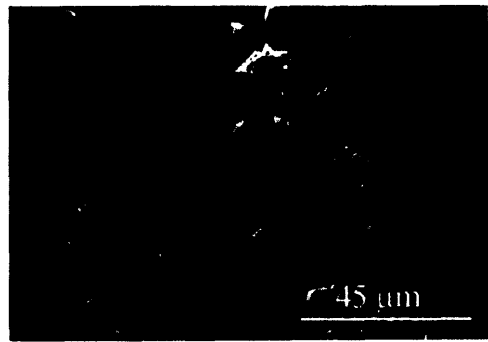


Fig. 21 Surface fracture behavior of nWC-15%Co during scratch test

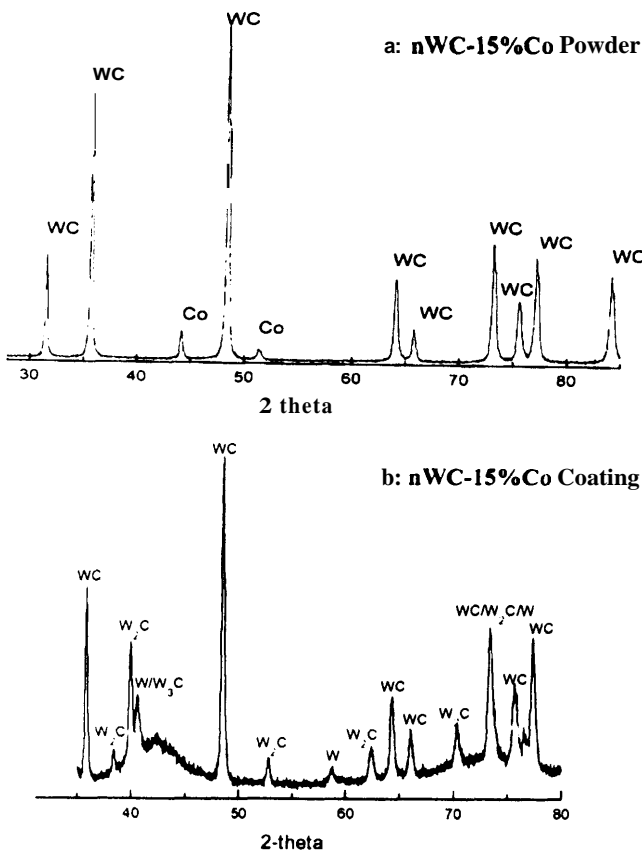


Fig. 20 XRD patterns on the nWC-15%Co (a) powder and (b) coating indicates the decomposition of WC to W_2C , W_3C phases

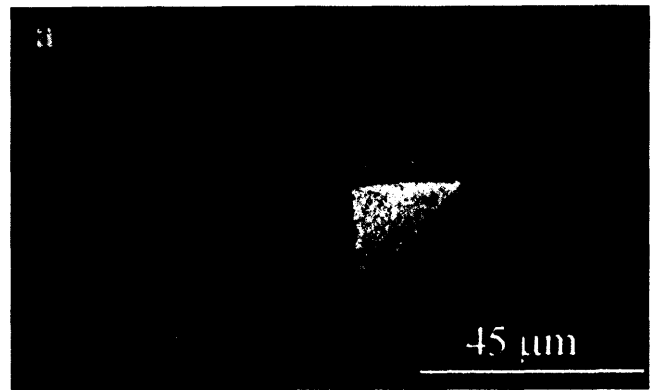


Fig. 22 Indentation fracture behavior of nWC-15%Co cross section. (a) Secondary and (b) backscattered electron images show interlamellar crack propagation.

3) and W_2C , W_3C phases (Ref 2). In laboratory tests, the presence of these phases has been shown to increase the propensity to fracture in thermal spray WC-Co coatings (Ref 2, 4). Such behavior is not characteristic of sintered WC-Co. Hence, the abrasion performance of thermal spray WC-Co is strongly related to relative fracture toughness (Ref 2, 4), while that of sintered WC-Co is strongly related to hardness (Ref 1). Therefore, it is important to investigate the effect of processing parameters on the level of decomposition of the nanostructured WC-Co during the thermal spray process. Furthermore, the effect of such decomposition on the fracture and tribological behavior of nWC-Co coatings needs to be investigated.

This research activity has been initiated to determine optimal HVOF processing parameters for producing dense and hard nWC-Co coatings. The powder examined here was nWC-15%Co (median powder size was $34 \mu\text{m}$) supplied by Nanodyne Inc., New Brunswick, NJ. The processing system used was the 2000 HV HVOF system supplied by Praxair Surface Technologies, Appleton, WI. The fuel gases were propylene at 66 slpm and oxygen at 263 slpm. The carrier gas was nitrogen at 38 slpm with a feed rate of 17 g/min. A 19 mm air cap was used to deposit coatings onto mild steel substrates placed at 250 mm from the nozzle end of the HVOF system. The coatings were examined for cross-sectional integrity by optical microscopy, for micro-

hardness by Vickers indentation at 300 g load, for **cross-sectional** fracture behavior by Vickers indentation at a 15 N load, and for surface fracture behavior by scratch tests with a Vickers indenter sliding at 250 $\mu\text{m/s}$ under a 20 N normal load. The results of these **examinations** are given in the figures summarized below.

The **nWC-15%Co** coatings produced were hard ($\text{HV}_{300}=1250$ to 1350) and displayed a dense microstructure (Fig. 19). The WC in the powder had undergone significant decomposition to W_2C (Fig. 20) as well as significant dissolution of W and C in the matrix, as apparent from the extent of amorphous phase distribution in the **nWC-Co** coating. The surface (Fig. 21) and cross-sectional (Fig. 22) fracture behavior of the coatings displayed interlamellar fracture, and crack propagation has been observed in other thermal spray WC-Co coatings (Ref 2, 4). The

surface fracture behavior indicates plastic deformation representative of ductile fracture behavior.

References

1. S.F. Wayne, J.G. Baldoni, and S.-T. Buljan, Abrasion and Erosion of WC-Co with Controlled Microstructures, *Tribol. Trans.*, Vol 33 (No. 4), 1990, p 611-617
2. S. Usmani, S. Sampath, D. Houck, and D. Lee. Effect of Carbide Grain Size on the Sliding and Abrasive Wear Behavior of Thermally Sprayed WC-Co Coatings, *Tribol. Trans.*, Vol 40 (No. 3), 1997, p 470-478
3. J.R. Fincke, W.D. Swank, and D.C. Haggard, Comparison of the Characteristics of HVOF and Plasma Thermal Spray, *Thermal Spray Industrial Applications*, C.C. Berndt and S. Sampath, Ed., ASM International, 1994, p 325-330
4. S. Usmani, "Abrasion and Sliding Friction of Thermal Spray Coatings," Ph.D. dissertation, 1997, SUNY at Stony Brook, NY

24. Complementarity of Experimental and Simulation Studies of Nanocrystalline Materials

J.A. Eastman and P. Keblinski, Argonne National Laboratory, IL, USA, jeastman@anl.gov

While experimentalists have studied nanocrystalline materials for more than fifteen years (Ref 1), it is only recently that significant efforts have been made to investigate their structures and properties via computer simulations. For example, Phillpot, Wolf, and Gleiter (Ref 2) recently developed a new molecular-dynamics simulation method for synthesis of fully dense nanocrystalline materials. Their techniques have been applied to studies of a **polycrystalline fcc** model material (Ref 2, 3) and to nanocrystalline silicon (Ref 4). The proceedings of a Materials Research Society Symposium "Nanophase and Nanocomposite Materials" (Ref 5) contains reports from several other groups employing simulation techniques to investigate the behavior of nanocrystalline materials.

Computer simulations provide information that is often complementary to that obtained from experimental studies. Simulation studies have advantages that include full control over microstructures, knowledge of precise atomic positions, and the ability to study high-temperature properties. On the other hand, experiments have advantages compared to simulation studies in that real materials are studied, **there** are no limits to sample size, and long-time scales are accessible.

A combined experimental-simulation approach was used to investigate the structure of nanocrystalline Pd (Ref 6) to obtain insight into the structure of grain boundaries in nanocrystalline materials. This has been a controversial subject with early studies (Ref 7, 8) proposing that interfaces in nanocrystalline materials represent a new class of solid-state structure lacking both short- and long-range order. More recent studies have disputed this view (Ref 9-11) and have concluded that the boundaries in nanocrystalline materials do not differ fundamentally in nature

from those in coarser-grained materials, particularly if samples are examined after aging for at least two weeks at room temperature (Ref 12). A diffraction analysis was applied to a fully relaxed nanocrystalline Pd structure simulation and compared with experimental diffraction data from nanocrystalline Pd (Ref 9). Both experimental and simulated diffraction data were analyzed using identical procedures (described in Ref 6 and 9).

The main results of the diffraction analysis of experimental and simulated nanocrystalline Pd data are shown in Fig. 23. A significant amorphous component is indicated in the simulation data (Fig. 23a). A real-space analysis of the simulation data showed that the amorphous structure is localized to the grain boundaries, with all boundaries in the simulation cell having amorphous structures and similar excess energies with respect to the perfect crystal. In contrast, no evidence of an amorphous phase is seen in the experimental diffraction data (Fig. 23b). A possible explanation for this apparent discrepancy between the experimental and simulation results is related to the fact that the **misorientations** between neighboring grains in the simulation cell were chosen such that all grain boundaries have high energy. In contrast, experimentally, when nanocrystalline materials are formed by the gas condensation process (Ref 1), individual grains may have freedom to rotate and facet into low energy orientations. Support for the idea that a significant fraction of the boundaries in gas-condensed nanocrystalline **fcc** metals are of low energy comes from mechanical property and high-resolution microscopy studies (Ref 13). A conclusion of this study is that it is important to understand that in both experimental and simulation studies, the structures and properties of nanocrystalline materials are controlled by the particular processing tech-

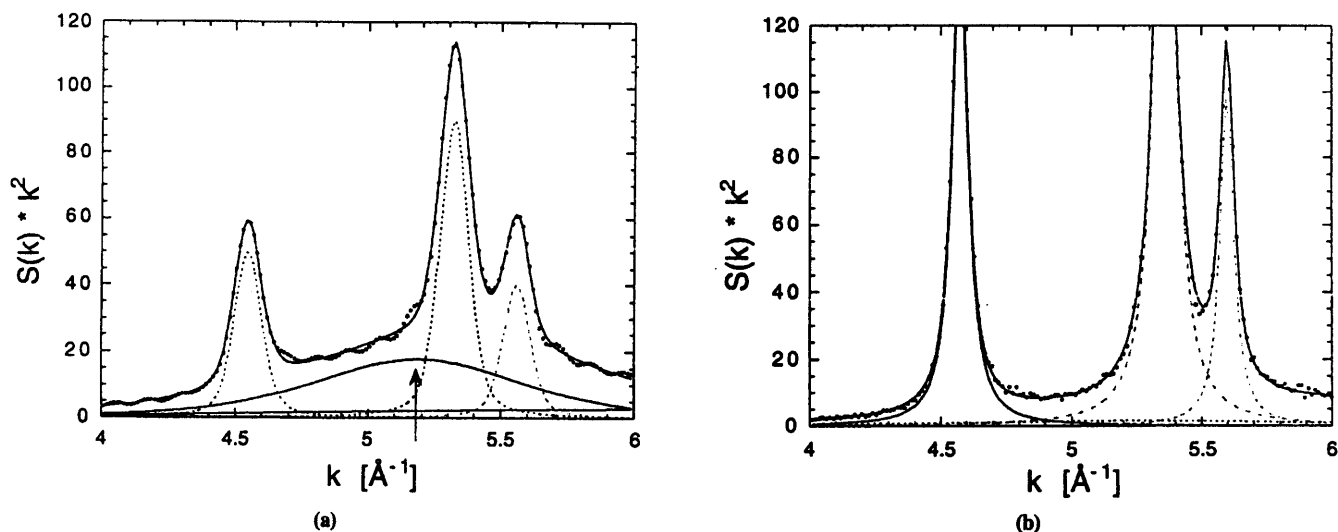


Fig. 23 (a) Simulation and (b) experimental nanocrystalline Pd diffraction data (points) with best fits (lines). In addition to the three crystalline Bragg peaks visible in the fit to the experimental data, an additional broad peak (arrow) is required to obtain a good fit to the simulation data. No evidence of an amorphous phase is seen in the experimental data.

niques employed. This will be important to remember in future studies of nanocrystalline materials produced by thermal spray techniques.

References

1. H. Gleiter, Mechanisms and Microstructures, *Deformation of Polycrystals*, Proc. 2nd Riso International Symposium on Metallurgy and Materials Science, 14-18 Sept 1981 (Roskilde, Denmark), Riso National Laboratory, 1981
2. S.R. Phillpot, D. Wolf, and H. Gleiter, Molecular-Dynamics Study of the Synthesis and Characterization of a Fully Dense, Three-Dimensional Nanocrystalline Material, *J. Appl. Phys.*, Vol 78 (No. 2), 1995, p 847-861
3. S.R. Phillpot, D. Wolf, and H. Gleiter, A Structural Model for Grain Boundaries in Nanocrystalline Materials, *Scr. Metall. Mater.*, Vol 33 (No. 8), 1995, p 1245-1251
3. P. Kebabinski, S.R. Phillpot, D. Wolf, and H. Gleiter, Amorphous Structure of Grain Boundaries and Grain Junctions in Nanocrystalline Silicon by Molecular-Dynamics Simulation, *Acta Mater.*, Vol 45 (No. 3), 1997, p 987-998
5. *Nanophase and Nanocomposite Materials II*, 2-5 December 1996 (Boston, MA). Symposium Proceedings, Vol 457, S. Komameni, J.C. Parker, and H.J. Wollenberger, Ed., Materials Research Society, 1997
6. P. Kebabinski and J.A. Eastman, in preparation
7. X. Zhu, R. Birringer, U. Hem, and H. Gleiter, X-Ray Diffraction Studies of the Structure of Nanometer-Sized Crystalline Materials, *Phys. Rev. B*, Vol 35 (No. 17), 1987, p 9085-9090
8. T. Haubold, R. Birringer, B. Lengeler, and H. Gleiter, EXAFS Studies of Nanocrystalline Materials Exhibiting a New Solid State Structure with Randomly Arranged Atoms, *Phys. Lett. A*, Vol 135 (No. 8-9), 1989, p 461-466
9. J.A. Eastman, M.R. Fitzsimmons, and L.J. Thompson, The Thermal Properties of Nanocrystalline Pd from 16 to 300 K, *Philos. Mag. B*, Vol 66 (No. 5), 1992, p 667-696
10. M.R. Fitzsimmons, J.A. Eastman, M. Muller-Stach, and G. Wallner, Structural Characterization of Nanometer-Sized Crystalline Pd by X-Ray Diffraction Techniques, *Phys. Rev. B*, Vol 44 (No. 6), 1991, p 2452-2460
11. G.J. Thomas, R.W. Siegel, and J.A. Eastman, Grain Boundaries in Nanophase Palladium: High Resolution Electron Microscopy and Image Simulation, *Scr. Metall. Mater.*, Vol 24 (No. 1), 1990, p 201-206
12. J. Löffler and J. Weissmüller, Grain-Boundary Atomic Structure in Nanocrystalline Palladium from X-Ray Atomic Distribution Functions, *Phys. Rev. B*, Vol 52 (No. 10), 1995, p 7076-7093
13. P.G. Sanders, M. Rittner, E. Kiedaisch, J.R. Weertman, H. Kung, and Y.C. Lu, Creep of Nanocrystalline Cu, Pd, and Al-Zr, *Nanostructured Mater.*, Vol 9 (No. 1-8), 1997, p 433-440

25. Fatigue Strength and Long-Term Thermal Aging of Ni-Base Superalloy Coatings

M. Okazaki, T. Sadasue, Y. Mutoh, M. Saitoh, and M. Okazaki,

Nagaoka University of Technology, Nagaoka, Japan, okazaki@mech.nagaokaut.ac.jp

As a part of a program to establish high-performance coating systems for blade and vane applications subjected to high temperatures in advanced gas turbines, the fatigue fracture of Ni-

base superalloy with different types of protective coatings was studied in comparison with that of the bare material, IN738LC. One was an overlay coated IN738LC with MCrAlY alloys (de-

noted by **MCrAlY/IN738LC**, where "M" represents Ni or Co), where two kinds of MCrAlY alloys—**CoNiCrAlY** and **CoCrAlY**—were employed. The other was **IN738LC** with two coatings in which an aluminide coating was additionally deposited onto the surface of **MCrAlY/IN738LC** (denoted by **Al_{CVD}/MCrAlY/IN738LC**). A 200 μm thick MCrAlY alloy was coated with **IN738LC** by **HVOF** spraying. As well, an aluminide coating of $\sim 5 \mu\text{m}$ thickness was deposited by a chemical vapor deposition (**CVD**) and is represented by **Al_{CVD}/MCrAlY/IN738LC**.

All fatigue tests were carried out at ambient temperature and 800 °C under load control at a frequency of 10 Hz and a loading ratio of 0.1, by means of an electrohydraulic fatigue testing machine. A main interest was to understand the fatigue strength of the coated specimens and the failure mechanisms relative to the uncoated material. It was shown that the fatigue lives of the **Al_{CVD}/MCrAlY/IN738LC** and those of the **MCrAlY/IN738LC** were significantly reduced in comparison to the uncoated material at room temperature, while a little reduction was observed at 800 °C (Fig. 24). Investigation of the fatigue crack initiation indicated that the early cracking in the aluminide layer, which consisted of brittle intermetallic phases of **NiAl** and **CoAl**, reduced the fatigue life of the **Al_{CVD}/MCrAlY/IN738LC**.

The MCrAlY alloy systems were also found to have a pronounced effect on the fatigue life of the coatings (Fig. 25). Furthermore, the influence of the long-term thermal aging for 2000 h at 900 °C on the fatigue properties was also studied, paying attention to the diffusion of alloying elements near the aluminide-layer/MCrAlY-coating interface and the MCrAlY-coating/substrate interface. Some noteworthy phenomena were found: The fatigue lives of the **MCrAlY/IN738LC** and **Al_{CVD}/MCrAlY/IN738LC** were extended a little and were not reduced by the application of thermal aging; however, adhesion between the **MCrAlY-coating** and the substrate was degraded. The fatigue failure mechanism can also be discussed by employing fracture mechanics to describe the crack initiation and propagation processes.

Selected References

- Y. Itoh, M. Saitoh, and M. Miyazaki, Mechanical Properties of Low-Pressure-Plasma-Sprayed MCrAlY Coatings, *J. Soc. Mater. Sci. Jpn.*, Vol 43, 1994, p 690-695 (in Japanese)
- Y. Itoh, M. Saitoh, and M. Miyazaki, Residual Stress Characteristics of High-Temperature Protective MCrAlY Coating, *Trans. Jpn. Soc. Mechanical Engineers*, Vol 60, 1994, p 141-146 (in Japanese)
- Y. Itoh, M. Saitoh, Y. Harada, and J. Takeuchi, Mechanical Properties of Aluminized MCrAlY Alloy Coatings, *J. Soc. Mater. Sci. Jpn.*, Vol 44, 1995, p 1361-1366 (in Japanese)
- M. Okazaki, T. Sadasue, M. Mutoh, and Y. Itoh, Fatigue Fracture Behavior of Ni-Base Superalloy **IN738LC** Coated with MCrAlY Alloys at High Temperatures, *J. Soc. Mater. Sci. Jpn.*, Vol 46, 1997, p 32-38 (in Japanese)
- T. Sadasue, M. Okazaki, M. Mutoh, and Y. Itoh, Fatigue Damage Process in MCrAlY Alloy Protective Coatings, *Localized Damage II!*, H. Nishitani, Ed., Computational Mechanics Publications, 1995, p 263-273

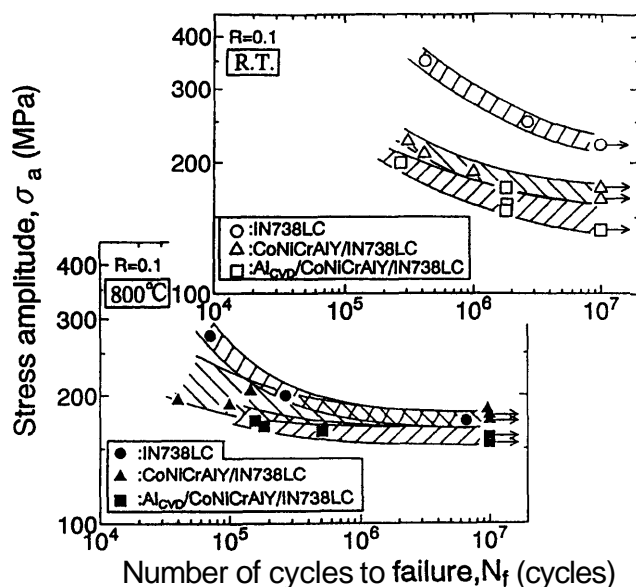


Fig. 24 Effect of the **CoNiCrAlY** alloy overlay coating and the duplex coating on the fatigue life of **IN738LC** Ni-base superalloy at room temperature and 800 °C

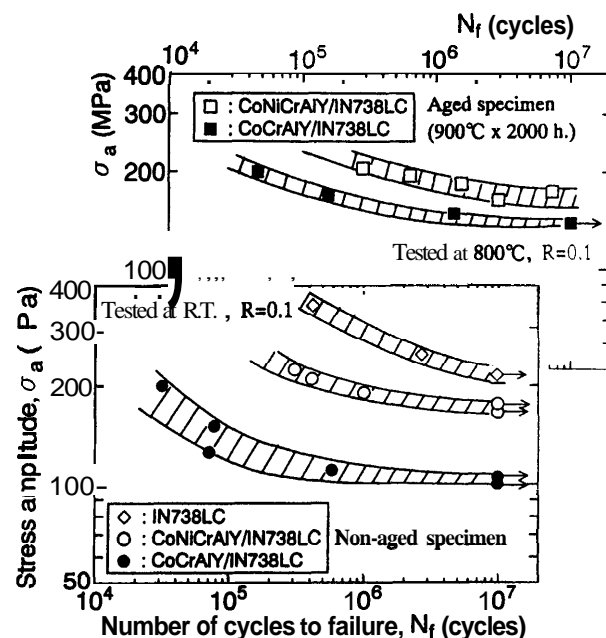


Fig. 25 Effect of MCrAlY alloy system on the fatigue lives of the overlay-coated **IN738LC**

T. Sadasue, K. Kubota, M. Okazaki, M. Mutoh, and M. Saitoh, Fatigue Strength of Aluminized Ni-Base Superalloys, *J. Mater. Test. Res. Assoc. Jpn.*, Vol 42, 1997, p 59-68 (in Japanese)

T. Sadasue, M. Okazaki, M. Mutoh, and M. Saitoh, Effect of Aluminide Coating on Fatigue Strength of a **CoNiCrAlY** Coated Ni-Base Superalloy at Ambient and High Temperatures, *Proc. Int. Conf. Materials and Mechanics*, H. Nakamura, Ed., Jpn. Soc. Mech. Eng., 1997, p 155-160

26. Microstructure and Mechanical Properties of WC/Co Nanocomposites

K. Jia and T.E. Fischer, Stevens Institute of Technology, NJ, USA, tfischer@stevens-tech.edu

The microstructure, mechanical properties, abrasion, and wear resistance of WC-Co nanocomposites synthesized by the spray conversion technique (Ref 1, 2) have been investigated and compared to the properties of conventional cermets. The binder phase of WC-Co nanocomposites is enriched in tungsten and carbon compared to conventional cermets. Small amorphous regions exist in the binder despite the slow cooling after liquid phase sintering. Few dislocations are found in the WC grains. The increased WC content and the amorphous regions strengthen the binder phase of the composites. Vickers indentation measurements agree with the known dependence on dislocation mean free path in the binder for conventional cermets and show a hardness reaching 2310 kg/mm² for the nanocomposites and ranging from 1100 to 1800 kg/mm² for conventional materials. While the toughness of conventional cermets decreases from 16 to 8 MPa√m with increasing hardness, the toughness does not decrease further as the WC grain size decreases from 0.7 to 0.07 μm, but remains constant at 8 MPa√m.

Scratches caused by a diamond indenter on nanocomposites are small, commensurate with their hardness. These scratches are ductile and devoid of the grain fracture that is observed with conventional materials. The abrasion resistance (Ref 3) of nanocomposites is about double that of the best conventional materials, although their hardness is larger by only 23% (Fig. 26). This is due to the absence, in the nanocomposites, of the WC grain fragmentation and removal that take place in conventional cermets. There is, therefore, a structural benefit to nanocomposites that goes beyond the increased hardness.

Sliding wear resistance (Ref 4) of WC/Co is proportional to hardness (Fig. 27); therefore, no additional benefit of a nanostructure is obtained. The appearance of the surfaces after sliding wear suggests a wear mechanism that has been observed also with Al₂O₃ and SiC; that is, the mechanical anisotropy of these hexagonal crystals allows material removal in the form of thin foils parallel to the easy gliding direction only. This also explains why the softer Si₃N₄, against which the cermets are rubbed, does not wear but is covered with a WC/Co sheet of transferred wear particles. The limited resolution of the scanning electron microscope, because of electron deflection by the magnetic field from the ferromagnetic Co phase, prevents the microscopic determination of the wear mechanisms in the nanophase materials.

References

1. L.E. McCandlish, B.H. Kear, and B.K. Kim, Chemical Processing of Nanophase WC/Co Composite Powders, *Mater. Sci. Technol.*, Vol 6, 1990, p 953-960
2. H. Fischmeister and H.E. Exner, Microstructure-Property Relations in WC-Co Alloys. *Arch. Eisenhüttenwes.*, Vol 37, 1966, p 499-524
3. K. Jia and T.E. Fischer, Abrasion Resistance of Nanostructured and Conventional Cemented Carbides, *Wear*; Vol 200, 1996, p 206-214
4. K. Jia and T.E. Fischer, Sliding Wear of Conventional and Nanostructured Cemented Carbides, *Wear*; Vol 203-204, 1997, p 310-318
5. S.B. Luyckx, F.R.N. Nabarro, S.-W. Wai, and M.N. James, The Anisotropic Work-Hardening of WC Crystals, *Acta Metall. Mater.*; Vol 40, 1992, p 1623-1627

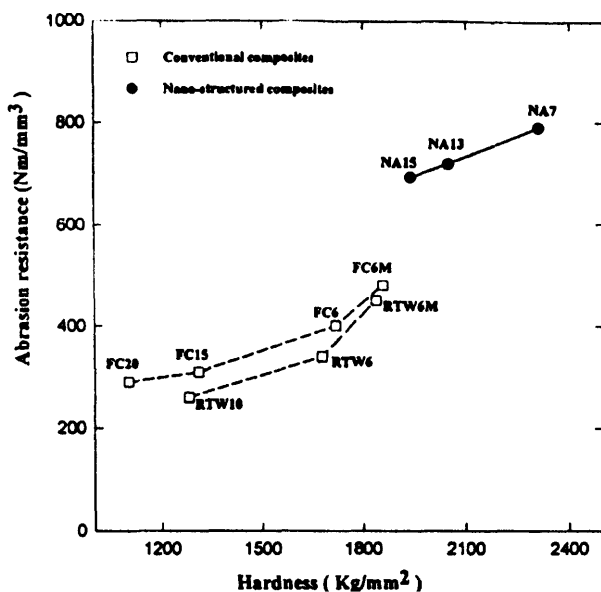


Fig. 26 Variation of resistance with hardness of WC-Co composites to abrasion by diamond. Full symbols represent nanocomposites, and open squares are for conventional cermets.

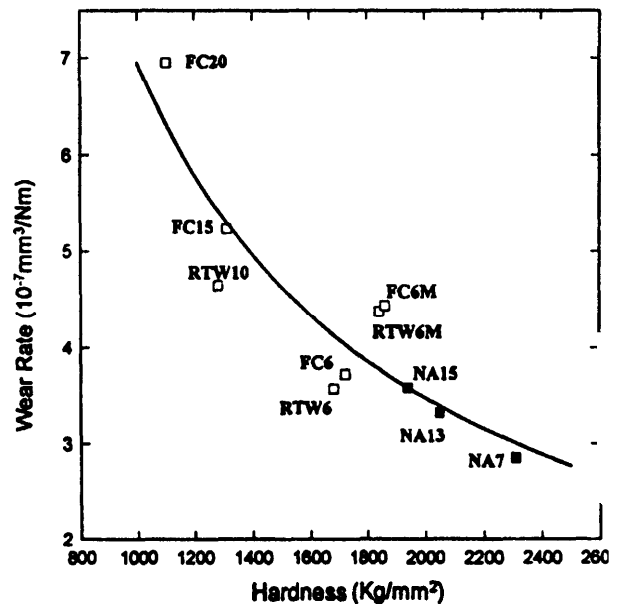


Fig. 27 Variation of the wear rate with hardness of WC-Co composites sliding against silicon nitride at 9.8 N applied load and 31.4 mm/s sliding speed

27. Synthesis and Thermal Stability Studies of Nanocrystalline Inconel 718 and Nickel Prepared by HVOF Thermal Spraying or Cryomilling

H.G. Jiang, M.L. Lau, and E.J. Lavernia, University of California at Irvine, CA, USA, lavernia@uci.edu

Nanocrystalline materials have engendered scientific and technical interest as a result of their unique structure, which in some instances has been documented to deliver unusual properties. Nanocrystalline materials inherently possess a significant fraction of high-energy, disordered grain boundary regions that

provide a strong driving force for grain growth. The ability to retain ultrafine grain sizes during hot consolidation or thermal spraying, however, is critical because it is precisely the fine grain size and large grain boundary volume that provide unique properties to the bulk material. Efforts directed in gaining insight into the mechanisms leading to superior thermal stability in nanocrystalline materials have been intensive in the past years.

In the present work, nanocrystalline Inconel 718 and Ni powders were prepared by methanol and cryogenic (in liquid nitrogen) attritor milling. Subsequent HVOF spraying of the methanol and cryogenic milled feedstock Inconel 718 powders enables various nanocrystalline Inconel 718 coatings to be found. Heat treatments were carried out to evaluate the thermal stability of methanol milled (Inconel 718) and cryomilled (Inconel 718 and Ni) powders, as well as the HVOF sprayed Inconel 718 coatings, respectively. It has been demonstrated that all of the Inconel 718 nanocrystalline powders and coatings studied herein exhibited superior thermal stability (Fig. 28). However, the thermal stability of HVOF sprayed coatings produced using methanol-milled Inconel 718 as feedstock powders is inferior to that of other Inconel 718 powders and coatings. The nanoscale carbides and oxides formed during milling were thought to be responsible for the superior thermal stabilities by inhibiting grain growth of the matrix grains via Zener pinning, although work in this area is continuing. In the case of the cryomilled nanocrystalline Ni powders, isothermal grain growth behavior was studied, from which the parameters required for predicting the evolution of microstructure using a nonisothermal annealing theory were acquired. A relatively good correspondence was observed between the experimental and the simulation results (see Fig. 29).

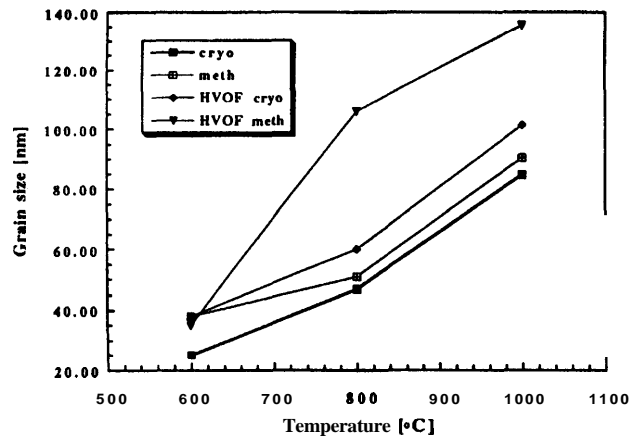


Fig. 28 Grain size versus annealing temperature (annealing time of 60 min) for cryomilled powders (cryo), methanol-milled powders (meth), HVOF sprayed cryomilled powders (HVOF cryo), and HVOF sprayed methanol-milled powders (HVOF meth)

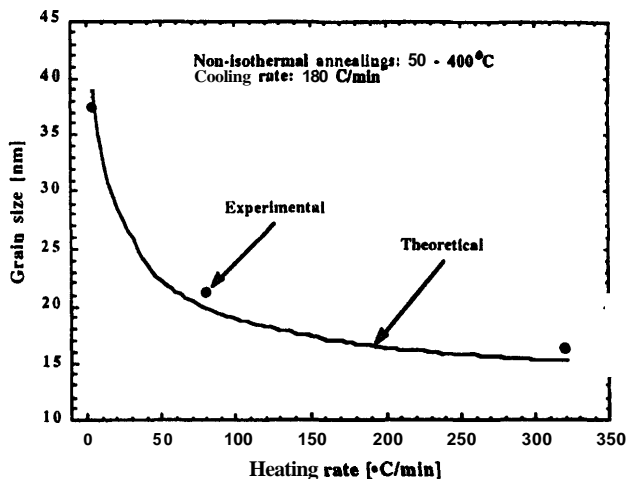


Fig. 29 Evolution of grain size as a function of heating rate. Solid circles represent the experimental results, while the solid line shows the simulation results.

Selected References

- D.L. Bourell and W. Kaysser, Effect of Nonisothermal Heating or Cooling on Grain Growth, *Acta Metall. Mater.*, Vol 41, 1993, p 2933-2937
- H. Gleiter, Nanocrystalline Materials, *Prog. Mater. Sci.*, Vol 33, 1989, p 223-315
- E.J. Lavernia, M.L. Lau, and H.G. Jiang, Thermal Spray Processing of Nanocrystalline Materials, presented in NATO ASI Conference, 1997 (St. Petersburg, Russia)
- V. Tellkamp, M.L. Lau, A. Fabel, and E.J. Lavernia, Thermal Spraying of Nanocrystalline Inconel 718, *Nanostructured Mater.*, Vol 9, 1997, p 489-492

28. Synthesis and Characterization of Nanocrystalline Nickel, Inconel 718, and 316 Stainless Steel Coatings

M.L. Lau, H.G. Jiang, and E.J. Lavernia, University of California at Irvine, CA, USA

This work describes the synthesis and characterization of nanocrystalline Ni, Inconel 718, and 316 stainless steel coatings. The feedstock powders were prepared by mechanical milling in which micrometer-sized powders were milled in either methanol or liquid nitrogen to produce flake-shaped agglomerates. The powders were introduced into the HVOF process to produce nanocrystalline coatings. The fuel-gas-to-oxygen ratio was varied to study how oxidation may affect the microstructure and properties of the coatings. X-ray diffraction analysis and transmission electron microscopy were used to determine the average grain size of the milled powders. Scanning electron microscopy was used to analyze the particle morphology as well as the microstructure of the coatings. In addition, coating properties of various materials were characterized by hardness measurements performed on the polished surface of the coating materials.

Figure 30 shows the morphological changes of Ni (99.5% purity) powders after 10 h of milling in methanol. The aspect ratio of milled powders determined by SEM analysis is 1.42. The average grain sizes determined by TEM dark-field imaging of methanol-milled Ni, Inconel 718, and 316 stainless steel powders for 10 h are 82, 16, and 24 nm, respectively. Results obtained from TEM dark-field imaging indicate that the average grain size decreases with increasing milling time for Ni, Inconel 718, and 316 stainless steel powders. For instance, the grain size

of a methanol-milled Ni (10 h) coating, determined by TEM dark-field imaging, is 100 to 200 nm, as shown in Fig. 31.

Backscattered electron images from SEM analysis performed on the as-sprayed nanocrystalline coatings show higher porosity present than those of conventional coatings with identical spraying parameters. Chemical composition analysis performed on the Ni coatings by EDAX indicates that the oxygen content of the Ni coating sprayed using air as the carrier gas is higher than that of the coating sprayed using N₂ as the carrier gas. Microhardness values of the thermal sprayed nanocrystalline Ni, Inconel 718, and 316 stainless steel coatings have been shown to be approximately 20%, 60%, and 36% higher than those of conventionally sprayed coatings.

Selected References

- E.J. Lavernia, H.G. Jiang, and M.L. Lau, "Thermal Spray Processing of Nanocrystalline Materials," presented at NATO Advanced Study Institute (ASI) on Nanostructured Materials: Science and Technology, 11-20 Aug 1997 (St. Petersburg, Russia)
- L. Pawlowski, *The Science and Engineering of Thermal Spray Coatings*, John Wiley & Sons, 1995
- V. Tellkamp, M.L. Lau, A. Fabel, and E.J. Lavernia, Thermal Spraying of Nanocrystalline Inconel 718, *Nanostructured Mater.*, Vol 9, 1997, p 489-492

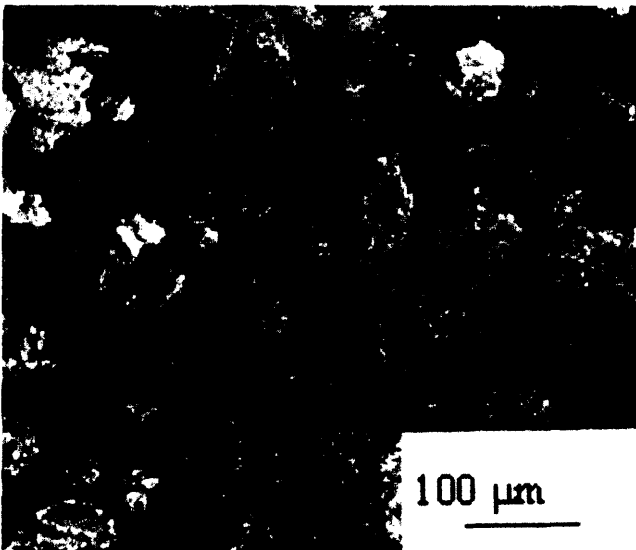


Fig. 30 Bright-field image of methanol-milled Ni (10 h) cross-sectional coating



Fig. 31 Dark-field image of methanol-milled Ni cross-sectional (10 h) coating

29. Processing of Nanostructured Ceramics and Bioceramics

J.Y. Ying, Massachusetts Institute of Technology, MA, USA, jyying@mit.edu

Nanostructured materials are of interest for a variety of structural, chemical, and functional applications. A forced-flow reactor for the large-scale synthesis of nanocrystalline materials has been developed. The reactor operates using a replenishable thermal evaporation source in a forced-gas flow. The gas stream can quickly remove particles generated from the hot-growth zone over the crucible to preserve the ultrafine particle size with minimal agglomeration. A downstream microwave-generated N_2 plasma allows in situ reaction of evaporated metals. A variety of nanocrystalline metals (Si and Al) and nitrides (Si_3N_4 , TiN, and AlN) have been produced with particle sizes of ~ 10 nm. The nitride nanoparticles produced in this reactor exhibit high quality. Their fine grain size, ultrahigh surface area (>200 m^2/g), and low agglomeration greatly facilitate densification. Careful handling/processing procedures that address the oxidation tendencies of the nanocrystalline nitrides were employed to produce

99% dense, nanostructured TiN (grain size ~ 250 nm) with a simple pressureless sintering process at $1400^\circ C$.

Nanocrystalline ceramic powders can also be generated by chemical routes. For example, metal salt, hydroxide, or alkoxide precursors are mixed with an aqueous base solution in chemical precipitation. Monodispersed colloidal particles of ~ 10 nm in diameter have been obtained through tuning the rate of hydrolysis precipitation by controlling sol composition, temperature, and pH. Nanocomposites of $Al_2O_3-ZrO_2$ and nanocrystalline hydroxyapatite of interest for thermal barrier coating and bioceramic applications, respectively, have been generated. These ultrafine powders are derived with excellent compositional homogeneity on the molecular level. The high-purity and ease of sintering of nanocrystalline powders derived from controlled precipitation contribute to stabilizing the desirable phase for superior mechanical performance and physical properties.

30. Characterization of Plasma Spray Coating in Spray Dried Cr_2O_3 Powder

**S.W. Lee and J.M. Park, Sun Moon University, Korea, swlee@omega.sunmoon.ac.kr, and
D.W. Lee and B.K. Kim, Korea Institute of Machinery and Materials, Korea**

Chromia powder was spray dried with different amounts of binder. The agglomerated particle sizes were studied to obtain the optimal plasma spray coating. The spray-dried Cr_2O_3 powders were sprayed onto a high-purity aluminum specimen (20 mm in diameter, 7 mm thick) by using the Metco MBN Gun of 40 kW. Plasma spray coating layers were investigated by varying the spray distance, gas flow rate, and gun current density. Mechanical properties such as hardness, surface roughness,

bonding strength, and wear resistance of the plasma spray coating layers on the aluminum disk were studied. The bonding strength between the sprayed coating layer and aluminum disk was measured using the ASTM C 633 method. The wear property was examined using the ball-on-plate reciprocal tribometer configuration. Also the thermal conductivity of the porous sprayed coating layers was measured by a noncontact flash temperature method.

31. Applications of Nanoporous Metal/Polymer Compounds

H.-G. Busmann, B. Guenther, and U. Meyer, Fraunhofer-Institut for Applied Materials Research (IFAM), Germany, bu@ifam-fhg.de

Novel nanoscale metal/polymer compounds in which a nanoporous metal powder is dispersed in an epoxy resin matrix have been produced by the following method. First, silver is evaporated in a vacuum chamber to form a supersaturated vapor in the presence of 2 to 5 mbar of an inert cooling gas like Ar or

He. Physical condensation and subsequent coalescence result in Ag nanoparticles. Then, the particles are deposited onto a substrate where they sinter together forming a spongy networklike nanoporous deposit. The deposit is taken out of the chamber and further processed by different methods of sieving and classifica-

tion. The final product is a powder with a **particle** size between 5 and 100 μm in which each particle forms a nanoporous network of high porosity.

One application of this powder is for electrically conductive adhesives for chip-on-board bonding. For this, the powder is dispersed in epoxy resins up to a concentration above the **perco-**

lation threshold. Due to the high porosity of each of the particles, this **threshold** is at about 7 **vol%** Ag compared with 22 **vol%** for the common **flake-filled** adhesives. Other prospective **applications** for these materials are in the fields of electromagnetic shielding, electrostatics, and polymer compounds with an increased thermal conductivity.

32. Applications for HVOF Thermal Sprayed Nanostructured Materials

R.W. Rigney, Integrated Systems Analysts, VA, USA, rigneybOisa.com

Thermal spray has been used to create solutions to corrosion and wear problems for more than ninety years. HVOF thermal spray has been developed over the last fifteen years as the best of these processes for applying metallic coatings. Nanostructured materials offer an increase in the utility of the HVOF process as a repair method and as a means to provide superior coatings for surface enhancement.

Many of the existing materials being used today provide an acceptable coating. These coatings are saving the end users

money in the form of less costly repair, faster turnaround, and longer service life. Many applications are rejected for consideration due to the limitations of thermal sprayed coatings. These limitations include inability to withstand point loads, excessive thermal expansion, low shear strength, and high crushing loads. The increase in physical properties that nanostructured materials will provide can enlarge the number and type of applications that are suitable for consideration.

33. The JRC Research Network on Nanostructured Materials

D.G. Rickerby and P. Fenici, Institute for Advanced Materials, European Commission Joint Research Centre, Italy, david.rickerby@jrc.it

The significant developments that have taken place in the nanostructured materials field since the beginning of this decade have progressed to a stage where the basic research activities are now giving way to the first potential commercial applications. Recognizing that this area is likely to have increasing economic as well as scientific impact, the Institute for Advanced Materials (IAM) has initiated a pilot project to establish a European Research Network on Nanostructured Materials.

The IAM has acquired appropriate expertise in this field through a program of experimental research on materials for structural and functional applications since 1991, including **r.f.** sputtered **c-BN** and **Ti-B-N** thin films for tribological applications, plasma sprayed partially stabilized zirconia thermal barrier coatings, and tin oxide gas sensors. A high-resolution TEM image of the microstructure of a magnetron-sputtered tin oxide film is shown in Fig. 32. Ongoing collaborations in **nanostructured** materials research include work with the Instituto de Fisica Aplicada, CSIC Madrid, on development of tin oxide and tita-

nium oxide solid-state gas sensors; Technical University of Denmark, Lyngby, on mechanical alloying in immiscible oxide systems; and **INRS—Énergie et Matériaux, Québec**, on nanocrystalline **Ti-Ru-Fe** alloys for electrocatalysis. Additional projects are being undertaken with the Naval Research Laboratory, Washington, on the improvement of mechanical properties of brittle alloys by nanostructural processing and the Department of Physics, University of Bologna, on high-vacuum mechanical milling of low-activation chromium alloys for fusion reactor structural applications.

The principal objective of the network is to identify key factors and important breakthroughs, assess the potential impact of new data, and provide a forum for an interchange of ideas and raising of consensus among experts from the scientific **community**. The proposed vehicle for communication will consist of a World Wide Web information exchange system. Members of the network will identify the main issues determining current and future developments, thereby defining a set of science and **tech-**



Fig. 32 High-resolution lattice plane image of magnetron sputtered tin oxide. (Specimen courtesy of M.C. Horrillo, CSIC Madrid). EELS mapping of the Fe distribution in mechanically alloyed 6 mol% SnO₂-Fe₂O₃ after 110 h milling. The mean grain size is approximately 10 nm. AFM image showing a three-dimensional view of the surface structure of an r.f. sputtered SnO₂ film on a polycrystalline alumina substrate. Integrated solid-state gas sensor for the detection of aromatic hydrocarbons fabricated on a single silicon chip. HREM image of an r.f. sputtered TiO_xN_y film evidencing a [0001] oriented, 20 nm diameter, a-titanium grain.

nology indicators to be subsequently monitored. Information will be distributed in the form of state-of-the-art reports and, whenever there is evidence that a critical point in the R&D cycle has been reached, additional actions may be organized such as topical workshops and conferences.

Selected References

- W. Gissler, J. Haupt, T.A. Crabb, P.N. Gibson, and D.G. Rickerby, Evidence for Mixed Phase Nanocrystalline Boron Nitride Films, *Mater. Sci. Eng.*, Vol A139, 1991, p 284-289
- W. Gissler, J. Haupt, A. Hoffmann, P.N. Gibson, and D.G. Rickerby, Mixed Phase Nanocrystalline Boron Nitride Films: Preparation and Characterization, *Thin Solid Films*, Vol 199, 1991, p 113-122
- J.Z. Jiang, R. Lin, K. Nielsen, S. Mørup, D.G. Rickerby, and R. Clasen, "Interstitial Positions of Tin Ions in α -(Fe,Sn)₂O₃ Solid Solutions Prepared by Mechanical Alloying," *Phys. Rev.*, Vol B55, 1997, p 14830-14835
- D.G. Rickerby, Microdiffraction Studies of Nanocrystalline Nitride Films, *Philos. Mag.*, Vol B68, 1993, p 939-948
- D.G. Rickerby, "Electron Microscopy Investigation of Grain Boundary and Planar Defect Structures in Nanocrystalline Oxides," NATO Advanced Study Institute on Nanostructured Materials, (St. Petersburg), 1997
- D.G. Rickerby, On the Grain Boundary and Defect Structure of Nanocrystalline Titanium Oxide, *Philos. Mag.*, 1997, in press
- D.G. Rickerby and T. Friesen, Microstructural Examination of Layered Coatings by Scanning Electron Microscopy, Transmission Electron Microscopy, and Atomic Force Microscopy, *Mater. Charact.*, Vol 36, 1996, p 213-223
- D.G. Rickerby, P.N. Gibson, W. Gissler, and J. Haupt, Structural Investigation of Reactively Sputtered Boron Nitride Films. *Thin Solid Films*, Vol 209, 1992, p 155-160
- D.G. Rickerby, M.C. Horrillo, J.P. Santos, and P. Serrini, Microstructural Characterization of Nanograin Tin Oxide Gas Sensors, *Nanostructured Mater.*, Vol 9, 1997, p 43-52
- D.G. Rickerby, J.Z. Jiang, R. Lin, and S. Mørup, Transmission Electron Microscopy Studies of Mechanical Alloying in the Immiscible Fe₂O₃-SnO₂ System, ISMANAM-97 (Barcelona) 1997

34. Technology Assessment of Nanostructured Coatings

M. Gell, University of Connecticut, CT, USA, mgell@mail.ims.uconn.edu

Nanostructured coatings hold promise to become the next generation of high-performance coatings based on a variety of property improvements resulting from reducing microstructural features to the nanoscale (10⁻⁹ m), (Fig. 33) (Ref 1-3). Nanostructured metals and alloys exhibit higher strength and hardness, at the expense of toughness, as the grain size is reduced. Ceramics and cermets exhibit higher hardness and improved wear resistance as the defect size is reduced.

Nanostructured WC-Co coatings show increased hardness and wear resistance compared to conventional material (Ref 4). These improvements are associated with the reduced slip distance in the cobalt matrix and the reduced initial crack size associated with smaller WC carbides (Ref 5).

Nanostructured thermal barrier coatings (TBCs), applied by thermal spraying, have the potential for improved durability and reduced thermal conductivity. The improved durability derives from the enhanced "splat" boundary strength and the reduced thermal conductivity results from the reduced grain size and the optimized pore size (Fig. 34) (Ref 6).

It is possible to project a whole new family of high-performance, nanostructured coatings with greatly improved wear, erosion, corrosion, and thermal resistance. However, it must be recognized that this emerging technology is in its infancy and considerable work must be done before its potential can be realized. Critical areas for research and development include (1) large-scale manufacture of cost-effective nanostructured pow-

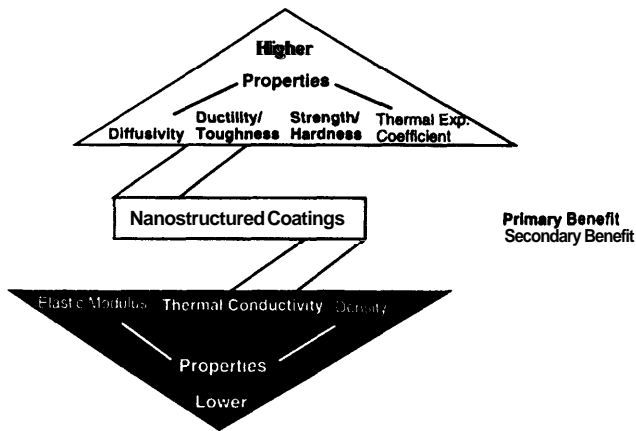


Fig. 33 Potential benefits of nanostructured coatings

der, (2) reconstitution of the nanoscale powders to sprayable size, (3) optimization and control of thermal spray processes to produce nanostructured coatings with desired chemistry, and (4) demonstration of thermal stability for coatings intended for elevated-temperature service.

References

1. M. Gell, Applying Nanostructured Materials in Future Gas Turbine Engines, *JOM*, Vol 46, Oct 1994, p 30-33
2. M. Gell, Application Opportunities for Nanostructured Materials and Coatings, *Mater. Sci. Eng.*, Vol A204, 1995, p 246-251
3. M. Gell, The Potential for Nanostructured Materials in Gas Turbine Engines, *Nanosructured Mater.*, Vol 6, 1995, p 997-1000

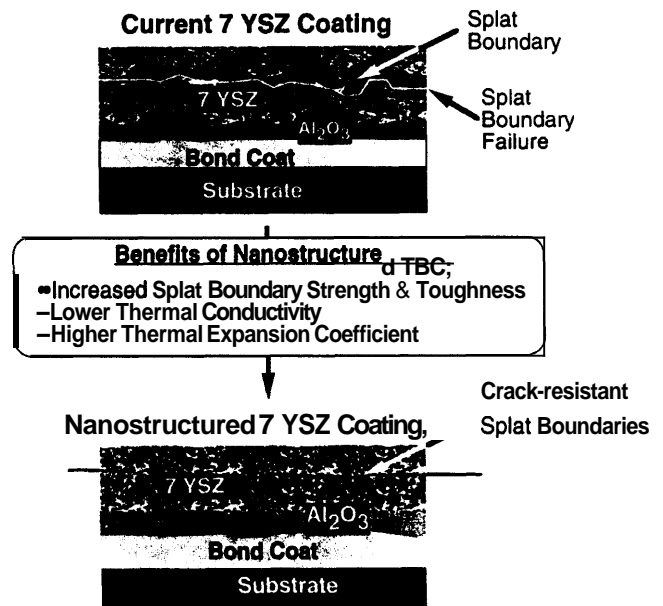


Fig. 34 Benefits of nanostructured thermal barrier coatings

4. B.H. Kear and P.R. Strutt, Nanostructures: The Next Generation of High Performance Bulk Materials and Coatings *Nav. Rev.*, Vol XLVI, 1994, p 4
5. T. Fischer. Tribological Aspects of Nanophase Materials. *Proc. Conf. Thermal Spray Processing of Nanoscale Materials*, Aug 1997 (Davos, Switzerland), *J. Therm. Spray Technol.*, to be published
6. P.G. Klemens and M. Gell, Thermal Conductivity of Thermal Barrier Coatings, Proc. of TBC Workshop, May 1997 (Cincinnati, OH), *Mater. Sci. Eng.*, to be published

Index of Authors

All authors have been indexed where the number refers to the abstract code.

Atteridge, D.	19	Jiang, H.G.	3, 27, 28	Okazaki, M.	25
Barrera , E.V.	18	Karhikeyan , J.	16	Park, J.M.	30
Becker, M.	19	Kawanaka, T.	14	Petrovicova, E.	20
Berndt, C.C.	16	Kear , B.H.	2, 7, 10	Provenzano , V.	18
Busmann, H.-G.	31	Kebliński , P.	24	Rawers , J.C.	21
Chen, Y.-J.	7, 10	Kim, B.K.	30	Rickerby, D.G.	33
Chraska, T.	16	Kim, G.E.	18	Rigney , R.W.	32
Cosandey, F.	7	King, A.H.	16	Ruhle, M.	11
Dent, A.H.	15	Knight, R.	20	Sadangi, R.	2
Eastman , J.A.	24	Koch , C.C.	22	Sadasue, T.	25
Eidelman, S.	9	Kujim, T.	14	Saito, N.	13
Fenici, P.	33	Kuriharai , L.	18	Saitoh, M.	25
Fischer, T.E.	26	Lau, M.L.	3, 27, 28	Sampath, S.	8, 23
Gell, M.	34	Lavernia, E.J.	3, 27, 28	Scholl, M.	19
Glumac, N.	7	Lee , D.W.	30	Shipway , P.H.	15
Glumac, N.G.	10	Lee, S.W.	30	Skandan, G.	2, 7, 10
Guenther, B.	31	McCartney , D.G.	15	Smith, M.F.	17
Hahn, H.	1	Meyer, U.	31	Smith, R.W.	20
Harris, S.J.	15	Miyamoto, Y.	14	Stewart, D.A.	15
Heims, E.	7	Murakami , K.	14	Strock , E.	5
Herman, H.	8, 23	Mutoh, Y.	25	Strutt, P.R.	4
Horlock, A.J.	15	Nakajima, H.	14	Trudeau, M.L.	6
Ishizaki, K.	12, 13	Nakamatsu, T.	13	Usmani, S.	23
Jia, K.	26	Nieser, R.A.	17	Ying, J.Y.	29

Acknowledgments: The editors acknowledge support from NSF Grant # CTS-93128% and MRSEC-NSF-DMR-9632570 (for CCB) and ONR Grant N00014-94-1-0017 (for **EJL**). Professor **E.J.** Lavernia also thanks the Alexander von Humboldt Foundation in Germany for support of his sabbatical visit at the Max-Planck-Institut für Metallforschung, in Stuttgart, Germany. The authors of abstracts #3, 27, 28 acknowledge financial support from the Office of Naval Research under grant No. N00014-94-1-0017. The authors of abstract #16 acknowledge NSF Grant # CTS-93128%. The authors of abstract #23 acknowledge support from the Office of Naval Research Advanced Coating Technology Development Program.